P_c IN MOLECULAR PICTURE

Kanokphon Phumphan

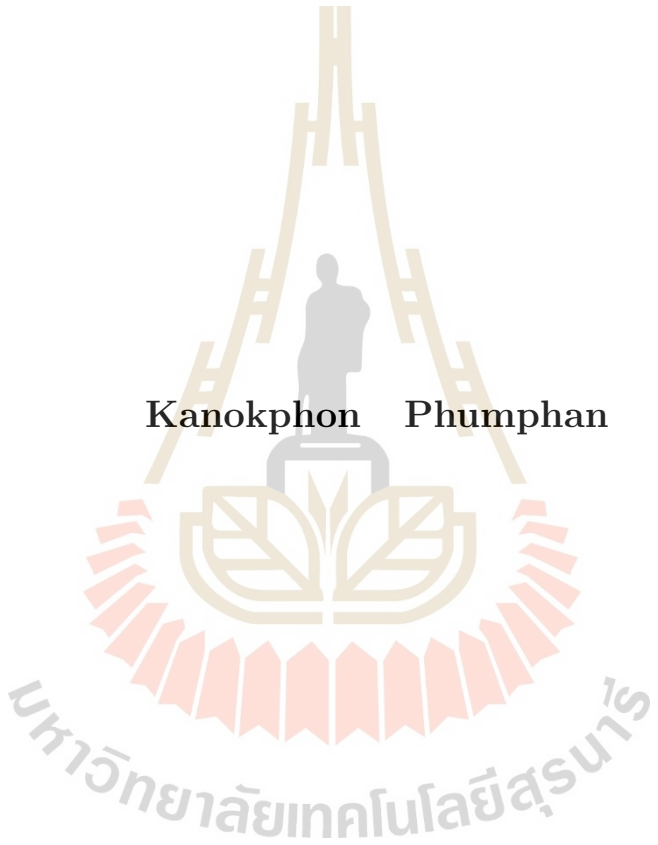

A Thesis Submitted in Partial Fulfillment of the Requirements for the

Degree of Master of Science in Physics

Suranaree University of Technology

Academic Year 2020

P_c ในรูปแบบการจำลองแบบโมเลกุล

นายกนกพล ภูมิพันธุ์

วิทยานิพนธ์นี้เป็นส่วนหนึ่งของการศึกษาตามหลักสูตรปริญญาวิทยาศาสตรมหาบัณฑิต

สาขาวิชาฟิสิกส์

มหาวิทยาลัยเทคโนโลยีสุรนารี

ปีการศึกษา 2563

P_c IN MOLECULAR PICTURE

Suranaree University of Technology has approved this thesis submitted in partial fulfillment of the requirements for a Master degree.

Thesis Examining Committee

(Assoc. Prof. Dr. Yi Yang)
Chairperson

(Prof. Dr. Yupeng Yan)
Member (Advisor)

(Asst. Prof. Dr. Ayut Limphirat)
Member (Co-Advisor)

(Prof. Dr. Chia-Chu Chen)
Member (Co-Advisor)

(Asst. Prof. Dr. Christoph Herold)
Member

(Assoc. Prof. Flt. Lt. Dr. Kontorn Chamniprasart)
Vice Rector for Academic Affairs and Internationalization

(Assoc. Prof. Dr. Worawat Meevasana)
Dean of Institute of Science

กนกพล ภูมิพันธุ์ : P_c ในรูปแบบการจำลองแบบโมเลกุล (P_c IN MOLECULAR PICTURE).
อาจารย์ที่ปรึกษา : ศาสตราจารย์ ดร.ยูเป็ง แยน, 58 หน้า

วิทยานิพนธ์นี้ได้ทำการศึกษาสถานะเพนตะควาร์กที่มีลักษณะคล้ายชาร์มโมเนียมในรูปแบบการจำลองแบบโมเลกุลระหว่างแบริออนและมีซอนบนกรอบการคำนวณของควาร์กโมเดล โดยพิจารณาทุกการจัดเรียงตัวของเพนตะควาร์กในสถานะพื้นที่เป็นไปได้ ซึ่งในวิทยานิพนธ์นี้ได้คำนวณหาค่าอัตราส่วนความกว้างของการสลายตัวของ $P_c(4312)$, $P_c(4440)$ และ $P_c(4457)$ ในทุก ๆ การจัดเรียงตัวที่เป็นไปได้ดังกล่าว ซึ่งผลจากความกว้างการสลายตัวแสดงให้เห็นว่า ทุกสถานะของเพนตะควาร์กที่สลายตัวไปสู่ช่องการสลายตัวเป็นโปรตอนและ J/ψ สำหรับ $J^P=1/2^-$ ล้วนสลายตัวไปสู่ช่องการสลายตัวเป็นโปรตอนและ η_c นอกจากนี้ ยังพบว่ามี 5 สถานะของเพนตะควาร์กในการจัดเรียงของสีแบบซิงเกลตที่สลายตัวในช่องการสลายตัวเป็นชาร์มแบบเปิดมีค่าสูงกว่าการสลายตัวในช่องการสลายตัวเป็นชาร์มแบบซ่อนและทุกสถานะของเพนตะคาร์กในการจัดเรียงตัวของสีแบบออกเตตอาจไม่สลายตัวในช่องการสลายตัวเป็นชาร์มแบบเปิด ซึ่งอาจสรุปได้ว่า เพนตะควาร์กในรูปแบบการจำลองแบบโมเลกุลระหว่างแบริออนและมีซอนมีค่าความกว้างการสลายตัวมากเมื่อการสลายตัวเป็นชาร์มแบบเปิด

สาขาวิชาฟิสิกส์ ลายมือชื่อนักศึกษา _____
ปีการศึกษา 2563 ลายมือชื่ออาจารย์ที่ปรึกษา _____
ลายมือชื่ออาจารย์ที่ปรึกษาร่วม _____
ลายมือชื่ออาจารย์ที่ปรึกษาร่วม _____

KANOKPHON PHUMPHAN : P_c IN MOLECULAR PICTURE
THESIS ADVISOR : PROF. YUPENG YAN, Ph.D. 58 PP.

HIDDEN-CHARM PENTAQUARK, CHARMONIUM-LIKE PENTAQUARK

We study charmonium-like pentaquarks in the baryon-meson molecule picture within the framework of the constituent quark model and consider all the possible configurations for the ground state of charmonium-like pentaquarks. The decay branch ratios of $P_c(4312)$, $P_c(4440)$ and $P_c(4457)$ are estimated for all the configurations and all possible decay channels. The decay patterns show that all the states decay in the pJ/ψ channel while all the states of $J^P = 1/2^-$ decay in the $p\eta_c$ channel. It is found that five states in the color *singlet* $\otimes$ *singlet* configuration decay in open charm channels dominantly over hidden charm channels, and all the states in the color *octet* $\otimes$ *octet* configuration may not decay in open charm channels. We may conclude that the baryon-meson molecules decay dominantly through open charm channels.

School of Physics
Academic Year 2020

Student's Signature _____
Advisor's Signature Yupeng Yan
Co-advisor's Signature _____
Co-advisor's Signature Chia Chu Chen

ACKNOWLEDGEMENTS

I would like to express my deep gratitude to Professor Yupeng Yan, Assistant Professor Ayut Limphirat and Professor Chia-Chu Chen, my research supervisors, for their patient guidance, enthusiastic encouragement and useful critiques of this research work. I would also like to thank Dr. Kai Xu and Atthaphon for their advices and assistances. My grateful thanks are also extended to Center of Excellence in High Energy Physics and Astrophysics, Suranaree University of Technology (SUT) and National Cheng Kung University (NCKU) for funding and providing the opportunity in this research. My special thanks are extended to the staff of the school of Physics, SUT for their supporting and coordination. Finally, I wish to thank my parents and my friends for their support and encouragement throughout my study.

Kanokphon Phumphan

CONTENTS

CONTENTS (Continued)

LIST OF TABLES

LIST OF TABLES (Continued)

LIST OF FIGURES

CHAPTER I

INTRODUCTION

1.1 Quark model and Exotic states

Quantum Chromodynamics (QCD) is the theory of the strong interaction. At present, it is still impossible to derive the hadron spectrum from the QCD Lagrangian analytically. The phenomenological models became one of the alternative approaches to study the strong interaction (Chen et al., 2016). The confinement property of QCD ensures that quarks and gluons are confined in hadrons. In 1964, Gell-Mann and Zweig independently developed the quark model (Gell-Mann, 1964; Zweig, 1964). The model successfully describes hadrons in the light quark sector which include u, d and s quarks, forming $SU(3)$ flavor symmetry with spin 1/2 for each quark. The quark model predicted the existence of Ω^- which composites of three strange quarks and was successfully discovered experimentally in 1964 (Barnes et al., 1964). In 2003, a candidate of pentaquark $\Theta^+(1540)$ has been observed (Nakano et al., 2003). However, it was not observed in a more precise measurement (Zhu, 2004). Since 2003, many exotic states such as charmonium-like and bottomonium-like states have been observed. These states have been studied in various theoretical models and experiments (Hosaka et al., 2016; Chen et al., 2016; Liu et al., 2019; Brambilla et al., 2020). Some of them cannot be fitted theoretically to the models (Chen et al., 2016; Brambilla et al., 2020).

1.2 The hidden charm pentaquark P_c

In 2015, Large Hadron Collider beauty (LHCb) reported the first discovery of a pentaquark in the decay of $\Lambda_b^0 \to pJ/\psi K^-$ in pp collision at center-of-mass

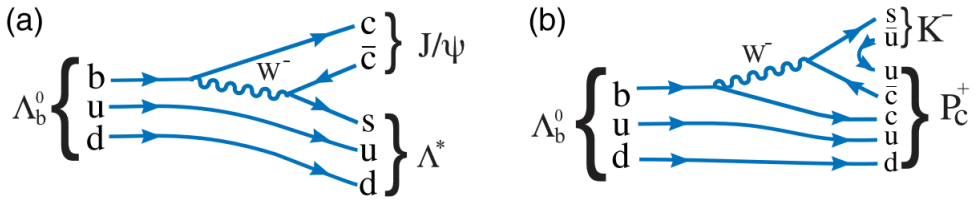

Figure 1.1 Feynman diagram of two possible intermediate states a) $\Lambda^* \to pK^-$ b) $P_c^+ \to pJ/\psi$ (Aaij et al., 2015).

energies of 7 and 8 TeV which corresponding to an integrated luminosity of 3 fb^{-1}(Aaij et al., 2015). The decay was expected to be dominated by $\Lambda_b^0 \to \Lambda^* J/\psi$ process as shown in Figure 1.1a. However, the experimental result shows that the Λ_b^0 decay via $P_c K^-$ channel significantly. According to the diagram in Figure 1.1b, the minimal quark content of the P_c state is $uudc\bar{c}$. Two pentaquark states were reported: $P_c(4380)$ and $P_c(4450)$. They have masses of $4380 \pm 8 \pm 29$ MeV and $4449.8 \pm 1.7 \pm 2.5$ MeV, with corresponding widths of $205 \pm 18 \pm 86$ MeV and $39 \pm 5 \pm 19$ MeV with statistical significances of 9σ and 12σ, respectively. The best fit of spin-parity J^P values are $\frac{3}{2}^-$ and $\frac{5}{2}^+$, respectively. The other acceptable J^P values are $(\frac{3}{2}^+, \frac{5}{2}^-)$ and $(\frac{5}{2}^+, \frac{3}{2}^-)$ (Aaij et al., 2015).

In 2019, LHCb reported the discovery of new P_c^+ states. An analysis of data from Run 1 and Run 2 at 13 TeV with to the integrated luminosity of 6 fb^{-1} shows that the $P_c(4450)$ is actually an overlap of two resonance peaks. It also revealed another resonance peak at 4312 MeV (Aaij et al., 2019).

The existence of the pentaquark states have been confirmed by ATLAS and D0 (Aaij et al., 2016; ATLAS collaboration, 2019; D0 Collaboration, 2019). Due to the broad peak of $P_c(4380)$, it has been pointed out by (Lü and Dong, 2016) that the resonance peak may be an overlap of resonances. In this work, we study only the three narrow pentaquark states which are given in Table 1.1.

Table 1.1 Summary of P_c states.

state	M [MeV]	Γ [MeV]	statistical significance
$P_c(4312)$	$4311.9 \pm 0.7^{+6.8}_{-0.6}$	$9.8 \pm 2.7^{+3.7}_{-4.5}$	7.3σ
$P_c(4440)$	$4440.3 \pm 1.3^{+4.1}_{-4.7}$	$20.6 \pm 4.9^{+8.7}_{-10.1}$	5.4σ
$P_c(4457)$	$4457.3 \pm 0.6^{+4.1}_{-1.7}$	$6.4 \pm 2.0^{+5.7}_{-1.9}$	5.4σ

1.3 Molecular picture

Interestingly, one notes that exotic quark states exist in the form of molecules of hadrons. One example is the deuteron which is a loosely bound state of a proton and a neutron with a binding energy of 2.2 MeV. The deuteron is an example for the molecule state which can be viewed as a composition of two color-singlet hadrons with a small binding energy. This inspired scientists to study the structures near the two-hadron threshold (Chen et al., 2016). LHCb results suggest molecular states for the three narrow P_c states as the masses of $P_c(4312)$ and $P_c(4457)$ are close to $\Sigma_c^+ \bar{D}^0$ and $\Sigma_c^+ \bar{D}^{*0}$ thresholds, respectively, while the mass of $P_c(4440)$ is about 20 MeV below $\Sigma_c \bar{D}^*$ mass threshold (Aaij et al., 2019) as shown in Figure 1.2.

Although there are many studies about these pentaquark states, their structures are still under investigation. So far, the decay of P_c has been observed only in the pJ/ψ channel. One should expect that other processes might be observed in future experiments. In this work, we study the hidden charm pentaquark with the assumption that the structure is a molecule state by using the quark model. We considered all the possible configuration of the ground state of hidden charm pentaquark. We also worked out all possible strong decay channels of $P_c(4312)$, $P_c(4440)$ and $P_c(4457)$.

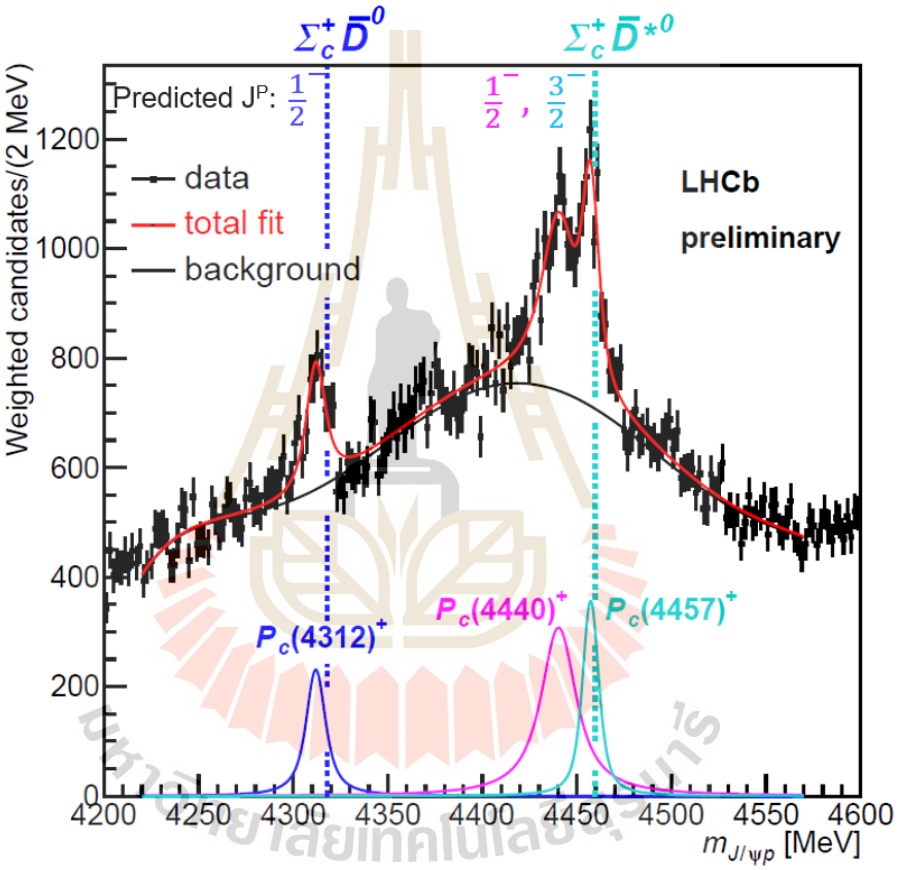

Figure 1.2 The narrow P_c states and $\Sigma_c^+\bar{D}^0$ and $\Sigma_c^+\bar{D}^{*0}$ mass thresholds with the correspond J^P values (Aaij et al., 2019).

CHAPTER II

P_C AND FINAL STATE WAVE FUNCTIONS

In this chapter, we show the derivation of configuration and wave function of both the pentaquark and all possible final states by applying group theory. We obtained the explicit wave function according to the symmetry in the configuration. We show all the possible configurations and quantum numbers for the pentaquark states in Section 2.2 and for the final states in Section 2.3. In this work, we used Young tabloids to present the irreducible representation of the permutation group S_n and special unitary group $SU(n)$ where the details can be found in Appendix A.1.

2.1 Configuration

The minimal quark content of P_c^+ is $uudc\bar{c}$ which is a positive charge state. In this work, we consider that the light quark q including u, d and s have the flavor symmetry of $SU(3)$, while the charm quark c and the anticharm quark $\bar{c}$ are not included in the flavor symmetry. The color of quarks are in the fundamental representation of $SU(3)_c$ while the color of anticharm quark $\bar{c}$ transforms under the conjugate fundamental representation. The construction scheme of wave functions follows two principles :

1. Due to the quark confinement picture, the pentaquark wave function should be a color singlet.

2. Since quarks are spin $\frac{1}{2}$ particles, the permutation of any light quark in the pentaquark wave function should be totally antisymmetric.

As we assumed that the pentaquark is in the baryon-meson molecule state, the color singlet should be constructed from baryon and meson. There are two possibilities of the color singlet configuration which are $singlet_B \otimes singlet_M$ and $octet_B \otimes octet_M$ where B and M refer to the baryon part and meson part, respectively. For the quark content in each molecule, we study only the case that the pentaquark is a molecule of charmed baryon $[qqc]$ and charmed meson $[q\bar{c}]$ since these quarks configurations are possible only in the molecular picture. The two possible configurations in the color degree of freedom are

$$\psi^c_{[111]}(qqc) \otimes \psi^c_{[111]}(q\bar{c}) = \begin{array}{|c|}\hline \\ \hline \\ \hline \\ \hline \end{array} \otimes \begin{array}{|c|}\hline \\ \hline \\ \hline \\ \hline \end{array}, \tag{2.1}$$

and

$$\psi^c_{[21]}(qqc) \otimes \psi^c_{[21]}(q\bar{c}) = \begin{array}{|c|c|}\hline \\ \hline \multicolumn{1}{|c}{} \\ \cline{1-1} \end{array} \otimes \begin{array}{|c|c|}\hline \\ \hline \multicolumn{1}{|c}{} \\ \cline{1-1} \end{array}, \tag{2.2}$$

where the configuration of Eq. (2.1) and Eq. (2.2) are called as color *singlet* $\otimes$ *singlet* configuration and color *octet* $\otimes$ *octet* configuration, respectively. [111] and [21] are the Young tabloid representations for the color singlet and octet, respectively where the [21] representation has two possibilities: mixed symmetric (or so-called λ type, symmetric for the first two particles) and mixed antisymmetric (or so called ρ type, antisymmetric for the first two particles) (see Appendix A.1).

2.1.1 Baryon part configuration

In this work, we study the pentaquark in the baryon-meson molecule state, the symmetry of the identical particle should be separately calculated in each molecule. Since the quarks in the meson part are not identical, so the meson wave function does not have to be antisymmetric. The baryon wave function has to be antisymmetric under the permutation of any light quark in the baryon. The total

wave function of the baryon part could be expressed in terms of

$$\Psi^B = \psi^{color}\eta^{spatial}\phi^{flavor}\chi^{spin}, \tag{2.3}$$

The quarks in the baryon part are $[qqc]$, so the wave function of baryon part should be antisymmetric for the first two light quarks. The total wave function of baryon part in the combination of color wave function ψ^{color} and spatial-spin-flavor wave function ψ^{osf} can be written as

$$\Psi^B = \sum_{i,j} a_{i,j}\psi^{color}_{[\lambda_c]_i}\psi^{osf}_{[\lambda_{osf}]_j}, \tag{2.4}$$

where $\psi^{osf} = \eta^{spatial}\phi^{flavor}\chi^{spin}$ with $[\lambda_{osf}]$ as a representation for the spatial-spin-flavor part where o stands for orbital referring to the spatial contribution. $[\lambda_c]$ could be [111] for the color $singlet \otimes singlet$ configuration or [21] for the color $octet \otimes octet$ configuration. The summation indices i and j depend on the representations. The coefficient $a_{i,j}$ can be determined by applying the permutation operator (see Appendix A.3). According to Eq. (2.4), the baryon wave function of the color $singlet \otimes singlet$ configuration can be written by

$$\Psi^B_{[111]} = \psi^{color}_{[111]}\psi^{osf}_{[2]}(q^2)c, \tag{2.5}$$

where c is the charm quark. While the total wave function of baryon part for the color $octet \otimes octet$ configuration has two possible cases:

$$\Psi^B_{[21]_\lambda} = \psi^{color}_{[21]_\lambda}\psi^{osf}_{[11]}(q^2)c, \tag{2.6}$$

and

$$\Psi^B_{[21]_\rho} = \psi^{color}_{[21]_\rho}\psi^{osf}_{[2]}(q^2)c. \tag{2.7}$$

Similar to Eq. (2.4), we can find the combination of ψ^{osf} in terms of $\eta^{spatial}$ and ψ^{sf}. The ψ^{osf} and ψ^{sf} can be written in the general form by

$$\psi^{osf}_{[\lambda_{osf}]} = \sum_{i,j} b_{i,j} \eta^{spatial}_{[\lambda_o]_i} \psi^{sf}_{[\lambda_{sf}]_j}, \tag{2.8}$$

$$\psi^{sf}_{[\lambda_{sf}]} = \sum_{l,m} c_{l,m} \phi^{flavor}_{[\lambda_f]_i} \chi^{spin}_{[\lambda_s]_j}. \tag{2.9}$$

We applied the orthogonal theorem of group theory to find the possible configurations for Eqs. (2.8) and (2.9) (see Appendix A.2). The orthogonal theorem in group theory leads to the following property for the characters of a group

$$\chi(g) = \sum_{\sigma} m_{(\sigma)} \chi^{(\sigma)}(g), \tag{2.10}$$

$$m_\sigma = \frac{1}{n} \sum_{g} \chi^{(\sigma)*}(g) \chi(g), \tag{2.11}$$

where g are group elements, $\chi(g)$ are the characters of a reducible representation and $\chi^{(\sigma)}(g)$ are the characters of the irreducible representation labeled by σ. The sum over σ is over all the irreducible representations of the group while the sum over g is over all the group elements. By applying Eq. (2.10), the irreducible representations $[\lambda_o]$, $[\lambda_{sf}]$, $[\lambda_s]$ and $[\lambda_f]$ are derived following the formula (Yan, 2020; Xu et al., 2019; James and Liebeck, 2001),

$$m_{[\lambda_{osf}]} = \sum_{i}^{r} \frac{\rho_i}{n} \chi_i^{[\lambda_{osf}]*} (\chi_i^{[\lambda_o]} \chi_i^{[\lambda_{sf}]}), \tag{2.12}$$

$$m_{[\lambda_{sf}]} = \sum_{i}^{r} \frac{\rho_i}{n} \chi_i^{[\lambda_{sf}]*} (\chi_i^{[\lambda_s]} \chi_i^{[\lambda_f]}), \tag{2.13}$$

where the finite group G of order n has r conjugacy classes $C_i (i = 1, 2 \ldots r)$ with the number of elements in the conjugacy class C_i being ρ_i. One may derive all the possible $[\lambda_o] \otimes [\lambda_{sf}]$ and $[\lambda_s] \otimes [\lambda_s]$ products which lead to nonzero $m_{[\lambda_{osf}]}$ and $m_{[\lambda_{sf}]}$, respectively.

All the possible spatial-spin-flavor and spin-flavor configurations are shown in Tables 2.1 and 2.2, respectively.

Table 2.1 Spatial-spin-flavor configuration for baryon part.

Color *singlet* $\otimes$ *singlet* configuration	$[2]_{osf}$	$[2]_o \otimes [2]_{sf}$ $[11]_o \otimes [11]_{sf}$
Color *octet* $\otimes$ *octet* configuration	$[2]_{osf}$	$[2]_o \otimes [2]_{sf}$ $[11]_o \otimes [11]_{sf}$
	$[11]_{osf}$	$[2]_o \otimes [11]_{sf}$ $[11]_o \otimes [2]_{sf}$

Table 2.2 Spin-flavor configuration for baryon part.

$[2]_{sf}$	$[2]_f \otimes [2]_s$ $[11]_f \otimes [11]_s$
$[11]_{sf}$	$[2]_f \otimes [11]_s$ $[11]_f \otimes [2]_s$

From Table 2.1, the configurations in the combination of color, spatial and spin-flavor wave function are

$$\Psi^B_{[111]} = \psi^{color}_{[111]} \eta^{spatial}_{[3]} \left(\psi^{sf}_{[2]}(q^2) \otimes c \right), \tag{2.14}$$

$$\Psi^B_{[21]_\lambda} = \psi^{color}_{[21]_\lambda} \eta^{spatial}_{[3]} \left(\psi^{sf}_{[11]}(q^2) \otimes c \right), \tag{2.15}$$

$$\Psi^B_{[21]_\rho} = \psi^{color}_{[21]_\rho} \eta^{spatial}_{[3]} \left(\psi^{sf}_{[2]}(q^2) \otimes c \right). \tag{2.16}$$

The combinations of the possible configuration for spin-flavor wave function from the symmetry in Table 2.2 are shown in Table 2.3, where ϕ and χ are flavor and spin wave function, respectively.

The configurations in Table 2.2 show that there is more than one possible spin and flavor configuration for a spin-flavor wave function, thus we show all possible

Table 2.3 Combinations of spin-flavor wave function.

$\psi^{sf}_{[2]}(q^2)$	$\phi_{[2]}\chi_1$
	$\phi_{[11]}\chi_0$
$\psi^{sf}_{[11]}(q^2)$	$\phi_{[2]}\chi_0$
	$\phi_{[11]}\chi_1$

combinations in terms of the color, spin and flavor wave function explicitly in Table 2.4, where S, λ, ρ and A stand for symmetry of [3], $[21]_\lambda$, $[21]_\rho$ and [111], respectively, ψ and ϕ are the color and flavor wave function, $\chi_{\frac{3}{2}}$ and $\chi_{\frac{1}{2}}$ are the spin wave function for spin $\frac{3}{2}$ and spin $\frac{1}{2}$, respectively, and c is the charmed quark.

Table 2.4 Configuration of baryon part wave function.

Color *singlet* $\otimes$ *singlet* configuration	$\psi_A\phi_{[2]}\chi_{\frac{3}{2}}c$
	$\psi_A\phi_{[2]}\chi_{\frac{1}{2}}c$
	$\psi_A\phi_{[11]}\chi_{\frac{1}{2}}c$
Color *octet* $\otimes$ *octet* configuration	$\psi_\lambda\phi_{[2]}\chi_{\frac{1}{2}}c$
	$\psi_\lambda\phi_{[11]}\chi_{\frac{3}{2}}c$
	$\psi_\lambda\phi_{[11]}\chi_{\frac{1}{2}}c$
	$\psi_\rho\phi_{[2]}\chi_{\frac{3}{2}}c$
	$\psi_\rho\phi_{[2]}\chi_{\frac{1}{2}}c$
	$\psi_\rho\phi_{[11]}\chi_{\frac{1}{2}}c$

The explicit form of the wave function that corresponds to the symmetry in the configuration can be derived by using projection operators in the Yamanouchi framework. The projection operator takes the form

$$P^{[\lambda]}_{(r)} = \sum_i \langle [\lambda](r)|g_i|[\lambda](r)\rangle\, g_i, \tag{2.17}$$

where $|[\lambda](r)\rangle$ is the Yamanouchi basis function of the representation $[\lambda]$ of permutation group S_n and g_i is the group element of S_n (see Appendix A.1). The projection operators of the permutation groups of S_3 and S_2 are

$$P^S = 1 + (12) + (13) + (23) + (123) + (132), \tag{2.18}$$

$$P^\lambda = 1 + (12) - \frac{1}{2}(13) - \frac{1}{2}(23) - \frac{1}{2}(123) - \frac{1}{2}(132), \tag{2.19}$$

$$P^\rho = 1 - (12) + \frac{1}{2}(13) + \frac{1}{2}(23) - \frac{1}{2}(123) - \frac{1}{2}(132), \tag{2.20}$$

$$P^A = 1 - (12) - (13) - (23) + (123) + (132), \tag{2.21}$$

$$P^{[2]} = 1 + (12), \tag{2.22}$$

$$P^{[11]} = 1 - (12), \tag{2.23}$$

where P^S, P^λ, P^ρ and P^A are the projection operators of [3], $[21]_\lambda$, $[21]_\rho$, and [111], respectively. For example, the proton flavor wave functions ϕ_λ and ϕ_ρ read:

$$\begin{aligned} P^\lambda uud &= uud + uud - \frac{1}{2}duu - \frac{1}{2}udu - \frac{1}{2}udu - \frac{1}{2}duu \\ &= 2uud - udu - duu \end{aligned}$$

$$\therefore \phi_\lambda = \frac{1}{\sqrt{6}}(2uud - udu - duu) \tag{2.24}$$

$$\begin{aligned} P^\lambda udu &= udu - duu + \frac{1}{2}udu + \frac{1}{2}uud - \frac{1}{2}duu - \frac{1}{2}uud \\ &= \frac{3}{2}(udu - duu) \end{aligned}$$

$$\therefore \phi_\rho = \frac{1}{\sqrt{2}}(udu - duu) \tag{2.25}$$

All the wave functions of color, flavor and spin for permutation symmetry are shown in Tables 2.5, 2.6 and 2.7.

Table 2.5 Color wave function of baryon part.

ψ_A	$\frac{1}{\sqrt{6}}(rgb - grb + gbr - rbg + brg - bgr)$
ψ_λ	$\frac{1}{\sqrt{6}}(2rrg - rgr - grr)$
	$\frac{1}{\sqrt{6}}(grg + rgg - 2ggr)$
	$\frac{1}{\sqrt{6}}(2rrb - rbr - brr)$
	$\frac{1}{\sqrt{12}}(2rgb + 2grb - gbr - rbg - brg - bgr)$
	$\frac{1}{\sqrt{6}}(2ggb - gbg - bgg)$
	$\frac{1}{\sqrt{6}}(brb + rbb - 2bbr)$
	$\frac{1}{\sqrt{6}}(bgb + gbb - 2bbg)$
	$\frac{1}{\sqrt{4}}(rbg + brg - bgr - gbr)$
ψ_ρ	$\frac{1}{\sqrt{2}}(rgr - grr)$
	$\frac{1}{\sqrt{2}}(rgg - grg)$
	$\frac{1}{\sqrt{2}}(rbr - brr)$
	$\frac{1}{\sqrt{4}}(gbr + rng - brg - bgr)$
	$\frac{1}{\sqrt{2}}(gbg - bgg)$
	$\frac{1}{\sqrt{2}}(rbb - brb)$
	$\frac{1}{\sqrt{2}}(gbb - bgb)$
	$\frac{1}{\sqrt{12}}(2rgb - 2grb - gbr + rbg - brg + bgr)$

Table 2.6 Flavor wave function of baryon.

ϕ_S	$\left\vert S,1,\frac{3}{2},+\frac{3}{2}\right\rangle$	$=$	uuu
	$\left\vert S,1,\frac{3}{2},+\frac{1}{2}\right\rangle$	$=$	$\frac{1}{\sqrt{3}}(uud+udu+duu)$
	$\left\vert S,1,\frac{3}{2},-\frac{1}{2}\right\rangle$	$=$	$\frac{1}{\sqrt{3}}(udd+dud+ddu)$
	$\left\vert S,1,\frac{3}{2},-\frac{3}{2}\right\rangle$	$=$	ddd
ϕ_λ	$\left\vert \lambda,1,\frac{1}{2},+\frac{1}{2}\right\rangle$	$=$	$\frac{1}{\sqrt{6}}(2uud-udu-duu)$
	$\left\vert \lambda,1,\frac{1}{2},-\frac{1}{2}\right\rangle$	$=$	$\frac{1}{\sqrt{6}}(dud+udd-2ddu)$
ϕ_ρ	$\left\vert \rho,1,\frac{1}{2},+\frac{1}{2}\right\rangle$	$=$	$\frac{1}{\sqrt{2}}(udu-duu)$
	$\left\vert \rho,1,\frac{1}{2},-\frac{1}{2}\right\rangle$	$=$	$\frac{1}{\sqrt{2}}(udd-dud)$
$\phi_{[2]}$	$\left\vert [2],\frac{2}{3},1,+1\right\rangle$	$=$	uuc
	$\left\vert [2],\frac{2}{3},1,0\right\rangle$	$=$	$\frac{1}{\sqrt{2}}(udc+duc)$
	$\left\vert [2],\frac{2}{3},1,-1\right\rangle$	$=$	ddc
$\phi_{[11]}$	$\left\vert [11],\frac{2}{3},0,0\right\rangle$	$=$	$\frac{1}{\sqrt{2}}(udc-duc)$

Table 2.7 Spin wave function of baryon (where the spin $\frac{1}{2}$ has two types, λ for mixed symmetric and ρ for mixed antisymmetric).

$\chi_{\frac{3}{2}}$	$\left\vert S,\frac{3}{2},+\frac{3}{2}\right\rangle$	$=$	$\vert\uparrow\uparrow\uparrow\rangle$
	$\left\vert S,\frac{3}{2},+\frac{1}{2}\right\rangle$	$=$	$\frac{1}{\sqrt{3}}(\vert\uparrow\uparrow\downarrow\rangle+\vert\uparrow\downarrow\uparrow\rangle+\vert\downarrow\uparrow\uparrow\rangle)$
	$\left\vert S,\frac{3}{2},-\frac{1}{2}\right\rangle$	$=$	$\frac{1}{\sqrt{3}}(\vert\uparrow\downarrow\downarrow\rangle+\vert\downarrow\uparrow\downarrow\rangle+\vert\downarrow\downarrow\uparrow\rangle)$
	$\left\vert S,\frac{3}{2},-\frac{3}{2}\right\rangle$	$=$	$\vert\downarrow\downarrow\downarrow\rangle$
$\chi_{\frac{1}{2}}$	$\left\vert \lambda,\frac{1}{2},+\frac{1}{2}\right\rangle$	$=$	$\frac{1}{\sqrt{6}}(2\vert\uparrow\uparrow\downarrow\rangle-\vert\uparrow\downarrow\uparrow\rangle-\vert\downarrow\uparrow\uparrow\rangle)$
	$\left\vert \lambda,\frac{1}{2},-\frac{1}{2}\right\rangle$	$=$	$\frac{1}{\sqrt{6}}(\vert\downarrow\uparrow\downarrow\rangle+\vert\uparrow\downarrow\downarrow\rangle-2\vert\downarrow\downarrow\uparrow\rangle)$
$\chi_{\frac{1}{2}}$	$\left\vert \rho,\frac{1}{2},+\frac{1}{2}\right\rangle$	$=$	$\frac{1}{\sqrt{2}}(\vert\uparrow\downarrow\uparrow\rangle-\vert\downarrow\uparrow\uparrow\rangle)$
	$\left\vert \rho,\frac{1}{2},-\frac{1}{2}\right\rangle$	$=$	$\frac{1}{\sqrt{2}}(\vert\uparrow\downarrow\downarrow\rangle-\vert\downarrow\uparrow\downarrow\rangle)$

2.1.2 Meson configuration

The color configuration for the meson has been shown in Eqs. (2.1) and (2.2), and we assume that the molecule is in the ground state. In Table 2.8, we list all possible meson configuration where $\psi_{[111]}$ and $\psi_{[21]}$ are color wave function. The color, flavor and spin wave function of the meson part are shown in Table 2.9, 2.10 and 2.11, respectively.

Table 2.8 Configuration of meson.

Color *singlet* $\otimes$ *singlet* configuration	Color *octet* $\otimes$ *octet* configuration
$\psi_{[111]}\phi(q\bar{c})\chi_1$	$\psi_{[21]}\phi(q\bar{c})\chi_1$
$\psi_{[111]}\phi(q\bar{c})\chi_0$	$\psi_{[21]}\phi(q\bar{c})\chi_0$

Table 2.9 Color wave function of meson.

$\psi_{[111]}$	$\frac{1}{\sqrt{3}}(r\bar{r}+g\bar{g}+b\bar{b})$
$\psi_{[21]}$	$r\bar{b}$
	$g\bar{b}$
	$-r\bar{g}$
	$\frac{1}{\sqrt{2}}(r\bar{r}-g\bar{g})$
	$g\bar{r}$
	$-b\bar{g}$
	$b\bar{r}$
	$\frac{1}{\sqrt{6}}(r\bar{r}+g\bar{g}-2b\bar{b})$

Table 2.10 Flavor wave function of meson part.

$\phi(q\bar{c})$	$u\bar{c}$
	$d\bar{c}$

Table 2.11 Spin wave function of meson.

χ_1	$\|1,+1\rangle$	=	$\|\uparrow\uparrow\rangle$
	$\|1,+0\rangle$	=	$\frac{1}{\sqrt{2}}(\|\uparrow\downarrow\rangle + \|\downarrow\uparrow\rangle)$
	$\|1,-1\rangle$	=	$\|\downarrow\downarrow\rangle$
χ_0	$\|0,0\rangle$	=	$\frac{1}{\sqrt{2}}(\|\uparrow\downarrow\rangle - \|\downarrow\uparrow\rangle)$

2.2 The pentaquark wave function

Since we study the pentaquark in the molecule state, the pentaquark configuration is given by a direct product of the baryon and meson. While there is no required symmetry in this direct product for the spin and flavor part but the color wave function has to be a color singlet following Eqs. (2.1) and (2.2). The color *singlet* $\otimes$ *singlet* configuration is simple due to the direct product between singlets can give only the singlet representation. For the color *octet* $\otimes$ *octet* configuration, the singlet wave function can be derived as

$$\psi^{P_c}_{singlet} = \frac{1}{\sqrt{8}} \sum_i \psi^B_{[21]_i} \otimes \psi^M_{[21]_i}, \tag{2.26}$$

where $\psi^B_{[21]_i}$ and $\psi^M_{[21]_i}$ are the color wave function in [21] representation of baryon and meson part, however to construct a color singlet then the meson color wave function has to be a conjugate state to the color wave function of the baryon in Table 2.12.

The flavor and spin wave function of the pentquark can be calculated by coupling the flavor and spin wave function of each configuration, using the Clebsh-Gordan coefficient (see Appendices A.4 and A.5). We show all the possible configuration and the corresponding spin and isospin of pentaquark in Table 2.13.

Table 2.12 The baryon color wave function and their conjugation from the meson color wave function.

ψ_λ	ψ_ρ	ψ_M
$\frac{1}{\sqrt{6}}(2rrg - rgr - grr)$	$\frac{1}{\sqrt{2}}(rgr - grr)$	$b\bar{r}$
$\frac{1}{\sqrt{6}}(grg + rgg - 2ggr)$	$\frac{1}{\sqrt{2}}(rgg - grg)$	$b\bar{g}$
$\frac{1}{\sqrt{6}}(2rrb - rbr - brr)$	$\frac{1}{\sqrt{2}}(rbr - brr)$	$-g\bar{r}$
$\frac{1}{\sqrt{12}}(2rgb + 2grb$ $-gbr - rbg - brg - bgr)$	$\frac{1}{\sqrt{4}}(gbr + rng - brg - bgr)$	$\frac{1}{\sqrt{2}}(r\bar{r} - g\bar{g})$
$\frac{1}{\sqrt{6}}(2ggb - gbg - bgg)$	$\frac{1}{\sqrt{2}}(gbg - bgg)$	$r\bar{g}$
$\frac{1}{\sqrt{6}}(brb + rbb - 2bbr)$	$\frac{1}{\sqrt{2}}(rbb - brb)$	$-g\bar{b}$
$\frac{1}{\sqrt{6}}(bgb + gbb - 2bbg)$	$\frac{1}{\sqrt{2}}(gbb - bgb)$	$r\bar{b}$
$\frac{1}{\sqrt{4}}(rbg + brg - bgr - gbr)$	$\frac{1}{\sqrt{12}}(2rgb - 2grb$ $-gbr + rbg - brg + bgr)$	$\frac{1}{\sqrt{6}}(2b\bar{b} - r\bar{r} - g\bar{g})$

2.3 Decay particles

Possible quark contents for the decay particles are $[qqq][c\bar{c}]$ and $[qqc][q\bar{c}]$. Since the decay particles are independent of each other, the color wave function of each decay particle must be a color singlet. Thus the configuration for the color, spin and flavor parts of the decay particles for $[qqc][q\bar{c}]$ appears to be the same as the color *singlet* $\otimes$ *singlet* configuration of the pentaquark in Table 2.13. The configuration for $[qqq][c\bar{q}]$ corresponds to the conventional baryon and the charmonium. For the conventional baryon $[qqq]$, The possible configurations for the spatial-spin-flavor wave function are shown in Table 2.14.

The combination of color, spatial and spin-flavor wave function for the ground state of the conventional baryon can be written by

$$\Psi_{[111]} = \psi^{color}_{[111]}\eta^{spatial}_{[3]}\psi^{sf}_{[3]}. \tag{2.27}$$

Table 2.13 P_c configurations.

Pentaquark configuration	Baryon part		Meson part	Isospin	Spin
$\Psi_{[111]_C[2]_F[3]_S}$	$\psi_{[111]}\phi_{[2]}\chi_S$	$\otimes$	$\psi_{[111]}\phi(q\bar{c})\chi_{[2]}$	$\frac{3}{2},\frac{1}{2}$	$\frac{5}{2},\frac{3}{2},\frac{1}{2}$
$\Psi_{[111]_C[2]_F[3][11]_S}$	$\psi_{[111]}\phi_{[2]}\chi_S$	$\otimes$	$\psi_{[111]}\phi(q\bar{c})\chi_{[11]}$	$\frac{3}{2},\frac{1}{2}$	$\frac{3}{2}$
$\Psi_{[111]_C[2]_F[21][2]_S}$	$\psi_{[111]}\phi_{[2]}\chi_\lambda$	$\otimes$	$\psi_{[111]}\phi(q\bar{c})\chi_{[2]}$	$\frac{3}{2},\frac{1}{2}$	$\frac{3}{2},\frac{1}{2}$
$\Psi_{[111]_C[2]_F[21][11]_S}$	$\psi_{[111]}\phi_{[2]}\chi_\lambda$	$\otimes$	$\psi_{[111]}\phi(q\bar{c})\chi_{[11]}$	$\frac{3}{2},\frac{1}{2}$	$\frac{1}{2}$
$\Psi_{[111]_C[11]_F[21][2]_S}$	$\psi_{[111]}\phi_{[11]}\chi_\rho$	$\otimes$	$\psi_{[111]}\phi(q\bar{c})\chi_{[2]}$	$\frac{1}{2}$	$\frac{3}{2},\frac{1}{2}$
$\Psi_{[111]_C[11]_F[21][11]_S}$	$\psi_{[111]}\phi_{[11]}\chi_\rho$	$\otimes$	$\psi_{[111]}\phi(q\bar{c})\chi_{[11]}$	$\frac{1}{2}$	$\frac{1}{2}$
$\Psi_{[21]^\lambda_C[2]_F[21]^\rho[2]_S}$	$\psi_{[21]^\lambda}\phi_{[2]}\chi_\rho$	$\otimes$	$\psi_{[21]}\phi(q\bar{c})\chi_{[2]}$	$\frac{3}{2},\frac{1}{2}$	$\frac{3}{2},\frac{1}{2}$
$\Psi_{[21]^\lambda_C[2]_F[21]^\rho[11]_S}$	$\psi_{[21]^\lambda}\phi_{[2]}\chi_\rho$	$\otimes$	$\psi_{[21]}\phi(q\bar{c})\chi_{[11]}$	$\frac{3}{2},\frac{1}{2}$	$\frac{1}{2}$
$\Psi_{[21]^\lambda_C[11]_F[3][2]_S}$	$\psi_\lambda\phi_{[11]}\chi_S$	$\otimes$	$\psi_{[21]}\phi(q\bar{c})\chi_{[2]}$	$\frac{1}{2}$	$\frac{5}{2},\frac{3}{2},\frac{1}{2}$
$\Psi_{[21]^\lambda_C[11]_F[3][11]_S}$	$\psi_\lambda\phi_{[11]}\chi_S$	$\otimes$	$\psi_{[21]}\phi(q\bar{c})\chi_{[11]}$	$\frac{1}{2}$	$\frac{3}{2}$
$\Psi_{[21]^\lambda_C[11]_F[21]^\lambda[2]_S}$	$\psi_\lambda\phi_{[11]}\chi_\lambda$	$\otimes$	$\psi_{[21]}\phi(q\bar{c})\chi_{[2]}$	$\frac{1}{2}$	$\frac{3}{2},\frac{1}{2}$
$\Psi_{[21]^\lambda_C[11]_F[21]^\lambda[11]_S}$	$\psi_\lambda\phi_{[11]}\chi_\lambda$	$\otimes$	$\psi_{[21]}\phi(q\bar{c})\chi_{[11]}$	$\frac{1}{2}$	$\frac{1}{2}$
$\Psi_{[21]^\rho_C[2]_F[3][2]_S}$	$\psi_\rho\phi_{[2]}\chi_S$	$\otimes$	$\psi_{[21]}\phi(q\bar{c})\chi_{[2]}$	$\frac{3}{2},\frac{1}{2}$	$\frac{5}{2},\frac{3}{2},\frac{1}{2}$
$\Psi_{[21]^\rho_C[2]_F[3][11]_S}$	$\psi_\rho\phi_{[2]}\chi_S$	$\otimes$	$\psi_{[21]}\phi(q\bar{c})\chi_{[11]}$	$\frac{3}{2},\frac{1}{2}$	$\frac{3}{2}$
$\Psi_{[21]^\rho_C[2]_F[21]^\lambda[2]_S}$	$\psi_\rho\phi_{[2]}\chi_\lambda$	$\otimes$	$\psi_{[21]}\phi(q\bar{c})\chi_{[2]}$	$\frac{3}{2},\frac{1}{2}$	$\frac{3}{2},\frac{1}{2}$
$\Psi_{[21]^\rho_C[2]_F[21]^\lambda[11]_S}$	$\psi_\rho\phi_{[2]}\chi_\lambda$	$\otimes$	$\psi_{[21]}\phi(q\bar{c})\chi_{[11]}$	$\frac{3}{2},\frac{1}{2}$	$\frac{1}{2}$
$\Psi_{[21]^\rho_C[11]_F[21]^\rho[2]_S}$	$\psi_\rho\phi_{[11]}\chi_\rho$	$\otimes$	$\psi_{[21]}\phi(q\bar{c})\chi_{[2]}$	$\frac{1}{2}$	$\frac{3}{2},\frac{1}{2}$
$\Psi_{[21]^\rho_C[11]_F[21]^\rho[11]_S}$	$\psi_\rho\phi_{[11]}\chi_\rho$	$\otimes$	$\psi_{[21]}\phi(q\bar{c})\chi_{[11]}$	$\frac{1}{2}$	$\frac{1}{2}$

Table 2.14 Spatial-spin-flavor configuration for baryon part.

$[3]_{osf}$	$[3]_o \otimes [3]_{sf}$
	$[21]_o \otimes [21]_{sf}$
	$[111]_o \otimes [111]_{sf}$

The possible configurations of spin-flavor wave function for the conventional baryon are shown in Table 2.15.

Table 2.15 Spin-flavor configuration for baryon part.

$[3]_{sf}$	$[3]_f \otimes [3]_s$
	$[21]_f \otimes [21]_s$
$[21]_{sf}$	$[3]_f \otimes [21]_s$
	$[21]_f \otimes [3]_s$, $[21]_f \otimes [21]_s$
	$[111]_f \otimes [21]_s$
$[111]_{sf}$	$[21]_f \otimes [21]_s$
	$[111]_f \otimes [3]_s$

The meson in the conventional baryon channel is a $c\bar{c}$ pair with the configuration in the ground state of

$$|J/\psi\rangle = \psi_{[111]}\eta_{[2]}\phi(c\bar{c})\chi_1, \tag{2.28}$$

$$|\eta_c\rangle = \psi_{[111]}\eta_{[2]}\phi(c\bar{c})\chi_0. \tag{2.29}$$

The explicit wave function of the conventional baryon and open charm baryon are given by Tables 2.5, 2.6, and 2.7 and for the corresponding meson by Tables 2.9, 2.10 and 2.11. All the possible configurations of the final particles are shown in Table 2.16.

2.4 Spatial wave function

As shown in Eq. (2.14) and Table 2.8, the spatial wave functions have to be totally symmetric for the ground state in each molecule. We used the harmonic oscillator to approximate the interaction between quarks. The Hamiltonian takes the form,

$$H_{P_c} = H_B + H_M + H'(\vec{R}), \tag{2.30}$$

Table 2.16 Final particle configuration.

Final particles	Baryon part		Meson part	Total Isospin	Total spin
$\Delta^+ J/\psi$	$\psi_{[111]}\phi_{[3]}\chi_S$	$\otimes$	$\psi_{[111]}\phi(c\bar{c})\chi_{[2]}$	$\frac{3}{2}$	$\frac{5}{2}, \frac{3}{2}, \frac{1}{2}$
$\Delta^+ \eta_c$	$\psi_{[111]}\phi_{[3]}\chi_S$	$\otimes$	$\psi_{[111]}\phi(c\bar{c})\chi_{[11]}$	$\frac{3}{2}$	$\frac{3}{2}$
pJ/ψ	$\psi_{[111]}(\phi_\lambda\chi_\lambda + \phi_\rho\chi_\rho)/\sqrt{2}$	$\otimes$	$\psi_{[111]}\phi(c\bar{c})\chi_{[2]}$	$\frac{1}{2}$	$\frac{3}{2}, \frac{1}{2}$
$p\eta_c$	$\psi_{[111]}(\phi_\lambda\chi_\lambda + \phi_\rho\chi_\rho)/\sqrt{2}$	$\otimes$	$\psi_{[111]}\phi(c\bar{c})\chi_{[11]}$	$\frac{1}{2}$	$\frac{1}{2}$
$\Sigma_c^* \bar{D}^*$	$\psi_{[111]}\phi_{[2]}\chi_S$	$\otimes$	$\psi_{[111]}\phi(q\bar{c})\chi_{[2]}$	$\frac{3}{2}, \frac{1}{2}$	$\frac{5}{2}, \frac{3}{2}, \frac{1}{2}$
$\Sigma_c^* \bar{D}$	$\psi_{[111]}\phi_{[2]}\chi_S$	$\otimes$	$\psi_{[111]}\phi(q\bar{c})\chi_{[11]}$	$\frac{3}{2}, \frac{1}{2}$	$\frac{3}{2}$
$\Sigma_c \bar{D}^*$	$\psi_{[111]}\phi_{[2]}\chi_\lambda$	$\otimes$	$\psi_{[111]}\phi(q\bar{c})\chi_{[2]}$	$\frac{3}{2}, \frac{1}{2}$	$\frac{3}{2}, \frac{1}{2}$
$\Sigma_c \bar{D}$	$\psi_{[111]}\phi_{[2]}\chi_\lambda$	$\otimes$	$\psi_{[111]}\phi(q\bar{c})\chi_{[11]}$	$\frac{3}{2}, \frac{1}{2}$	$\frac{1}{2}$
$\Lambda_c^+ \bar{D}^*$	$\psi_{[111]}\phi_{[11]}\chi_\rho$	$\otimes$	$\psi_{[111]}\phi(q\bar{c})\chi_{[2]}$	$\frac{1}{2}$	$\frac{3}{2}, \frac{1}{2}$
$\Lambda_c^+ \bar{D}$	$\psi_{[111]}\phi_{[11]}\chi_\rho$	$\otimes$	$\psi_{[111]}\phi(q\bar{c})\chi_{[11]}$	$\frac{1}{2}$	$\frac{1}{2}$

where H_B and H_M are the Hamiltonian of baryon and meson, H' is a interaction Hamiltonian of the baryon and meson molecule. The harmonic oscillator of baryon and meson takes the form

$$H_A = \sum_i^N \frac{p_i^2}{2m_i} + \alpha_A \sum_{i<j}^N (\vec{r}_i - \vec{r}_j)^2, \tag{2.31}$$

where A is either baryon or meson, α_A is a force constant which is assumed to be the same for every quark in the molecule but different for each molecule of the baryon or meson. Under the flavor symmetry, u and d quark have the same mass m while charm quark has mass M. The Hamiltonian of the light quark baryon and the charmed baryon have the same forms in Jacobi coordinates but with different parameters,

$$H_{B_c} = \frac{p_\rho^2}{2m} + \frac{p_\lambda^2}{2\mu} + 3\alpha_{B_c}(\rho^2 + \lambda^2), \tag{2.32}$$

$$H_B = \frac{p_\rho^2}{2m} + \frac{p_\lambda^2}{2m} + 3\alpha_B(\rho^2 + \lambda^2), \tag{2.33}$$

$$\vec{\lambda} = \frac{1}{\sqrt{6}}(\vec{r}_1 + \vec{r}_2 - 2\vec{r}_3),$$
$$\vec{\rho} = \frac{1}{\sqrt{2}}(\vec{r}_1 - \vec{r}_2),$$
$$\mu = \frac{3mM}{2m + M}.$$

The Hamiltonian of charmed meson and light quark meson takes the form,

$$H_{\bar{D}} = \frac{p_\sigma^2}{2\mu'} + 2C_{\bar{D}}\xi^2, \tag{2.34}$$

$$H_M = \frac{p_\sigma^2}{2m} + 2C_M\xi^2, \tag{2.35}$$

$$\vec{\xi} = \frac{1}{\sqrt{2}}(\vec{r}_4 - \vec{r}_5),$$
$$\mu' = \frac{2mM}{m + M}.$$

The Hamiltonian in Eq. (2.32) and Eq. (2.34) can be used for both the pentaquark and the decay particles.

CHAPTER III

DECAY OF THE P_C

In this chapter, we show the calculation and results of the dynamical properties of the decay processes of the pentaquarks.

3.1 Transition amplitude

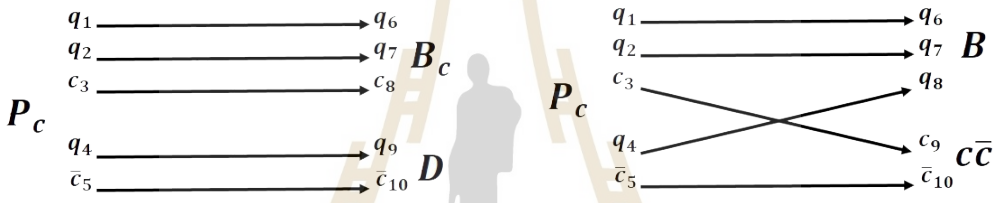

(a) Direct diagram O_S **(b)** Cross diagram O_C

Figure 3.1 Quark line diagrams.

We study the decay of pentaquark by using the quark interchange model with the quark line diagrams in Figure 3.1. From the diagrams, the transition amplitude of the decay should be written in the momentum space as

$$\begin{aligned} T_i = \int d^3p_1 \cdots d^3p_5 d^3p_6 \cdots d^3p_{10} \, \langle BM|\vec{p_6}\vec{p_7}\vec{p_8}\vec{p_9}\vec{p_{10}}\rangle \\ \langle \vec{p_6}\vec{p_7}\vec{p_8}\vec{p_9}\vec{p_{10}}|O_i|\vec{p_1}\vec{p_2}\vec{p_3}\vec{p_4}\vec{p_5}\rangle \\ \langle \vec{p_1}\vec{p_2}\vec{p_3}\vec{p_4}\vec{p_5}|P_c\rangle \, , \end{aligned} \tag{3.1}$$

where the operator O_i of the quark line diagrams takes the form

$$O_S = \lambda_S \delta^{(3)}(\vec{p}_1 - \vec{p}_6)\delta^{(3)}(\vec{p}_2 - \vec{p}_7)\delta^{(3)}(\vec{p}_3 - \vec{p}_8)\delta^{(3)}(\vec{p}_4 - \vec{p}_9)\delta^{(3)}(\vec{p}_5 - \vec{p}_{10}), \tag{3.2}$$

$$O_C = \lambda_C \delta^{(3)}(\vec{p}_1 - \vec{p}_6)\delta^{(3)}(\vec{p}_2 - \vec{p}_7)\delta^{(3)}(\vec{p}_3 - \vec{p}_9)\delta^{(3)}(\vec{p}_4 - \vec{p}_8)\delta^{(3)}(\vec{p}_5 - \vec{p}_{10}). \tag{3.3}$$

Following the spatial wave function of the pentaquark and final states, the transition amplitude is

$$T_i = T^O \cdot f^{CSF}, \tag{3.4}$$

where T^O is the transition amplitude in the spatial part and f^{CSF} is the color-spin-flavor factor,

$$f^{CSF} = \left\langle \psi_B^{CSF} \psi_M^{CSF} \middle| \psi_{P_c}^{CSF} \right\rangle. \tag{3.5}$$

We will show the color-spin-flavor factor values for every pentaquark configuration in open channel in Section 3.3.

The partial decay width for the pentaquark decay can be calculated by the two-body decay formula in the center of mass frame,

$$\Gamma = \int \frac{d^3p_B}{(2\pi)^3} \frac{d^3p_M}{(2\pi)^3} |T|^2 (2\pi)^4 \delta^{(3)}(\vec{p_B} + \vec{p_M}) \delta(E_{P_c} - E_B - E_M), \tag{3.6}$$

where $E_{B,M} = \sqrt{m_{B,M}^2 + \vec{p}_{B,M}^2}$. From the transition amplitude Eq. (3.4), the partial decay width takes the form

$$\Gamma = C^2 \lambda_i^2 \frac{E_B E_M}{M_{P_c}} f(q^2) \left| f^{CSF} \right|^2, \tag{3.7}$$

where $f(q^2)$ is the kinematic phase factor from the spatial part of T^O as a function of decay particle momentum $q = |P_B| = |P_M|$. Solving the transition amplitude of the spatial part T^O involves a lot of parameters which must be fit from experiment. A similar analytical calculation in $p\bar{p}$ collisions shows that the transition amplitude has the Gaussian form from the MIT bag model (Dover et al., 1992),

$$f(q^2) \approx q e^{-\alpha q^2 R^2}, \tag{3.8}$$

where R is the bag radius and α can be obtain via fitting to the experiment data. Here, the exponential arises from wave function overlap in the harmonic oscillator

approximation (Dover et al., 1992). Instead of using the analytic calculation of T^O, we introduce the phenomenological phase factor (Vandermeulen, 1988),

$$f(\sqrt{s}, m_B, m_M) = q(\sqrt{s}, m_B, m_M) \exp\left\{-A(s - s_{BM})^{1/2}\right\}, \tag{3.9}$$

where $q(\sqrt{s}, m_B, m_M) = \frac{1}{2m_{P_c}}\sqrt{(m_{P_c}^2 - (m_B + m_M)^2)((m_{P_c}^2 - (m_B - m_M)^2))}$, $s_{B,M} = (m_B + m_M)^2$ and $A = 1.2$ GeV^{-1}. We calculated the normalized partial decay width by choosing a reference decay channel. The normalized decay width is

$$\frac{\Gamma_i}{\Gamma_a} = \frac{E_{B_i} E_{M_i}/M_{P_{ci}}}{E_{B_a} E_{M_a}/M_{P_{ca}}} \frac{f(\sqrt{s}, m_{B_i}, m_{M_i})}{f(\sqrt{s}, m_{B_a}, m_{M_a})} \frac{\left|f_i^{CSF}\right|^2}{\left|f_a^{CSF}\right|^2}. \tag{3.10}$$

3.2 Momentum and Phenomenological form

We calculated the momentum of the final particles for each P_c and their open channels in Table 3.1 and $f(\sqrt{s}, m_B, m_M)$ values as defined in Eq. (3.9) in Table (3.2).

Table 3.1 Final particles momentum in MeV.

Final state	Final mass	$P_c(4312)$	$P_c(4440)$	$P_c(4457)$
$\Delta^+\eta_c$	4214	417.521	642.375	667.22
$p\eta_c$	3922	788.713	923.544	940.494
$\Delta^+ J/\psi$	4327	n/a	451.526	485.167
pJ/ψ	4035	658.118	809.443	828.059
$\Sigma_c^*\bar{D}$	4387	n/a	338.272	389.163
$\Sigma_c\bar{D}$	4322	n/a	503.93	539.569
$\Lambda_c^+\bar{D}$	4154	575.53	780.367	804.047
$\Sigma_c^*\bar{D}^*$	4529	n/a	n/a	n/a
$\Sigma_c\bar{D}^*$	4464	n/a	n/a	n/a
$\Lambda_c^+\bar{D}^*$	4296	185.173	559.699	592.4

Table 3.2 $f(\sqrt{s}, m_B, m_M)$ values.

Final state	$P_c(4312)$	$P_c(4440)$	$P_c(4457)$
$\Delta^+\eta_c$	139.412	119.937	116.89
$p\eta_c$	91.836	76.0007	74.1211
$\Delta^+ J/\psi$	n/a	136.762	134.581
pJ/ψ	106.134	87.6319	85.4071
$\Sigma_c^* \bar{D}$	n/a	148.87	151.384
$\Sigma_c \bar{D}$	n/a	148.749	146.114
$\Lambda_c^+ \bar{D}$	143.656	118.92	115.737
$\Sigma_c^* \bar{D}^*$	n/a	n/a	n/a
$\Sigma_c \bar{D}^*$	n/a	n/a	n/a
$\Lambda_c^+ \bar{D}^*$	118.623	145.69	142.544

3.3 Color-Spin-Flavor factor

From Eq. 3.3, we calculated the transition amplitude of color-spin-flavor f^{CSF}. Tables 3.3 and 3.4 show the f^{CSF} for the hidden charm decay channel which can proceed via both straight and cross diagrams while Table 3.5 for the open charm decay channel which can proceed only via the straight diagram.

Table 3.3 Color-Spin-Flavor factor of the $\Delta^+ J/\psi$ and $\Delta^+ \eta_c$ channel for $\mathbf{I} = \frac{3}{2}$.

j	P_c configuration	$\Delta^+ J/\psi$	$\Delta^+ \eta_c$
$\frac{5}{2}$	$\Psi_{[111]_C[2]_F[3][2]_S}$	0.1111	
	$\Psi_{[21]^\rho_C[2]_F[3][2]_S}$	0.8888	
$\frac{3}{2}$	$\Psi_{[111]_C[2]_F[3][2]_S}$	0.0034	0.0463
	$\Psi_{[111]_C[2]_F[3][11]_S}$	0.0462	0.0277
	$\Psi_{[111]_C[2]_F[21][2]_S}$	0.0617	0.0370
	$\Psi_{[21]^\rho_C[2]_F[3][2]_S}$	0.0246	0.3703
	$\Psi_{[21]^\rho_C[2]_F[3][11]_S}$	0.3703	0.0555
	$\Psi_{[21]^\rho_C[2]_F[21][2]_S}$	0.4938	0.0740
$\frac{1}{2}$	$\Psi_{[111]_C[2]_F[3][2]_S}$	0.0123	
	$\Psi_{[111]_C[2]_F[21][2]_S}$	0.0246	
	$\Psi_{[111]_C[2]_F[21][11]_S}$	0.0740	
	$\Psi_{[21]^\rho_C[2]_F[3][2]_S}$	0.0987	
	$\Psi_{[21]^\rho_C[2]_F[21][2]_S}$	0.1975	
	$\Psi_{[21]^\rho_C[2]_F[21][11]_S}$	0.5925	

Table 3.4 Color-Spin-Flavor factor of the pJ/ψ and $p\eta_c$ channel for $\mathbf{I} = \frac{1}{2}$.

j	P_c configuration	pJ/ψ	$p\eta_c$
$\frac{3}{2}$	$\Psi_{[111]_C[2]_F[3][2]_S}$	0.0308	
	$\Psi_{[111]_C[2]_F[3][11]_S}$	0.0185	
	$\Psi_{[111]_C[2]_F[21][2]_S}$	0.0061	
	$\Psi_{[111]_C[11]_F[21][2]_S}$	0.0555	
	$\Psi_{[21]^\rho_C[2]_F[3][2]_S}$	0.2469	
	$\Psi_{[21]^\rho_C[2]_F[3][11]_S}$	0.1481	
	$\Psi_{[21]^\rho_C[2]_F[21]^\lambda[2]_S}$	0.0493	
	$\Psi_{[21]^\rho_C[11]_F[21]^\rho[2]_S}$	0.4444	
$\frac{1}{2}$	$\Psi_{[111]_C[2]_F[3][2]_S}$	0.0123	0.0370
	$\Psi_{[111]_C[2]_F[21][2]_S}$	0.0385	0.0046
	$\Psi_{[111]_C[2]_F[21][11]_S}$	0.0046	0.0138
	$\Psi_{[111]_C[11]_F[21][2]_S}$	0.0.138	0.0416
	$\Psi_{[111]_C[11]_F[21][11]_S}$	0.0416	0.0138
	$\Psi_{[21]^\rho_C[2]_F[3][2]_S}$	0.0987	0.2962
	$\Psi_{[21]^\rho_C[2]_F[21]^\lambda[2]_S}$	0.3086	0.0370
	$\Psi_{[21]^\rho_C[2]_F[21]^\lambda[11]_S}$	0.0370	0.1111
	$\Psi_{[21]^\rho_C[11]_F[21]^\rho[2]_S}$	0.0123	0.3333
	$\Psi_{[21]^\rho_C[11]_F[21]^\rho[11]_S}$	0.3333	0.1111

Table 3.5 Color-Spin-Flavor factor of the open charm channel.

I	**j**	P_c configuration	$\Sigma_c^*\bar{D}^*$	$\Sigma_c\bar{D}^*$	$\Lambda_c^+\bar{D}^*$	$\Sigma_c^*\bar{D}$	$\Sigma_c\bar{D}$	$\Lambda_c^+\bar{D}$
$\frac{3}{2}$	$\frac{5}{2}$	$\Psi_{[111]_C[2]_F[3][2]_S}$	1					
$\frac{3}{2}$	$\frac{3}{2}$	$\Psi_{[111]_C[2]_F[3][2]_S}$	1					
		$\Psi_{[111]_C[2]_F[21][2]_S}$		1				
		$\Psi_{[111]_C[2]_F[3][11]_S}$				1		
$\frac{3}{2}$	$\frac{1}{2}$	$\Psi_{[111]_C[2]_F[3][2]_S}$	1					
		$\Psi_{[111]_C[2]_F[21][2]_S}$		1				
		$\Psi_{[111]_C[2]_F[21][11]_S}$					1	
$\frac{1}{2}$	$\frac{5}{2}$	$\Psi_{[111]_C[2]_F[3][2]_S}$	1					
$\frac{1}{2}$	$\frac{3}{2}$	$\Psi_{[111]_C[2]_F[3][2]_S}$	1					
		$\Psi_{[111]_C[2]_F[21][2]_S}$		1				
		$\Psi_{[111]_C[11]_F[21][2]_S}$			1			
		$\Psi_{[111]_C[2]_F[3][11]_S}$				1		
$\frac{1}{2}$	$\frac{1}{2}$	$\Psi_{[111]_C[2]_F[3][2]_S}$	1					
		$\Psi_{[111]_C[2]_F[21][2]_S}$		1				
		$\Psi_{[111]_C[11]_F[21][2]_S}$			1			
		$\Psi_{[111]_C[2]_F[21][11]_S}$					1	
		$\Psi_{[111]_C[11]_F[21][11]_S}$						1

3.4 Partial decay width ratio

In this subsection, the decay width ratios for the open channel of the same P_c configuration are evaluated. We find that the decay width ratios of the three P_c states are of the same magnitude. Thus we only show the results from $P_c(4457)$ in Tables 3.6 and 3.7.

Table 3.6 Partial width ratio of $P_c(4457)$ for $\mathbf{I} = \frac{3}{2}$.

j	P_c configuration	$\Delta^+\eta_c$	$p\eta_c$	Δ^+J/ψ	pJ/ψ	$\Sigma_c^*\bar{D}$	$\Sigma_c\bar{D}$	$\Lambda_c^+\bar{D}$	$\Lambda_c^+\bar{D}^*$
$\frac{5}{2}$	$\Psi_{[111]_C[2]_F[3][2]_S}$			1					
	$\Psi_{[21]^\rho_C[2]_F[3][2]_S}$			1					
$\frac{3}{2}$	$\Psi_{[111]_C[2]_F[3][2]_S}$	13.458		1					
	$\Psi_{[111]_C[2]_F[3][11]_S}$	0.537		1		28.507			
	$\Psi_{[111]_C[2]_F[21][2]_S}$	0.537		1					
	$\Psi_{[21]^\rho_C[2]_F[3][2]_S}$	13.44		1					
	$\Psi_{[21]^\rho_C[2]_F[3][11]_S}$	0.559		1					
	$\Psi_{[21]^\rho_C[2]_F[21]^\lambda[2]_S}$	0.537		1					
$\frac{1}{2}$	$\Psi_{[111]_C[2]_F[3][2]_S}$			1					
	$\Psi_{[111]_C[2]_F[21][2]_S}$			1					
	$\Psi_{[111]_C[2]_F[21][11]_S}$			1			17.275		
	$\Psi_{[21]^\rho_C[2]_F[3][2]_S}$			1					
	$\Psi_{[21]^\rho_C[2]_F[21]^\lambda[2]_S}$			1					
	$\Psi_{[21]^\rho_C[2]_F[21]^\lambda[11]_S}$			1					

Table 3.7 Partial width ratio of $P_c(4457)$ for $\mathbf{I} = \frac{1}{2}$.

j	P_c configuration	$\Delta^+\eta_c$	$p\eta_c$	$\Delta^+ J/\psi$	pJ/ψ	$\Sigma_c^*\bar{D}$	$\Sigma_c\bar{D}$	$\Lambda_c^+\bar{D}$	$\Lambda_c^+\bar{D}^*$
$\frac{3}{2}$	$\Psi_{[111]_C[2]_F[3][2]_S}$				1				
	$\Psi_{[111]_C[2]_F[3][11]_S}$				1	116.072			
	$\Psi_{[111]_C[2]_F[21][2]_S}$				1				
	$\Psi_{[111]_C[11]_F[21][2]_S}$				1				37.062
	$\Psi_{[21]^\rho_C[2]_F[3][2]_S}$				1				
	$\Psi_{[21]^\rho_C[2]_F[3][11]_S}$				1				
	$\Psi_{[21]^\rho_C[2]_F[21]^\lambda[2]_S}$				1				
	$\Psi_{[21]^\rho_C[11]_F[21]^\rho[2]_S}$				1				
$\frac{1}{2}$	$\Psi_{[111]_C[2]_F[3][2]_S}$		2.699		1				
	$\Psi_{[111]_C[2]_F[21][2]_S}$		0.107		1				
	$\Psi_{[111]_C[2]_F[21][11]_S}$		2.701		1		451.107		
	$\Psi_{[111]_C[11]_F[21][2]_S}$		2.698		1				148.317
	$\Psi_{[111]_C[11]_F[21][11]_S}$		0.299		1			39.964	
	$\Psi_{[21]^\rho_C[2]_F[3][2]_S}$		2.697		1				
	$\Psi_{[21]^\rho_C[2]_F[21]^\lambda[2]_S}$		0.109		1				
	$\Psi_{[21]^\rho_C[2]_F[21]^\lambda[11]_S}$		2.698		1				
	$\Psi_{[21]^\rho_C[11]_F[21]^\rho[2]_S}$		2.697		1				
	$\Psi_{[21]^\rho_C[11]_F[21]^\rho[11]_S}$		0.299		1				

3.5 Normalized decay width

Since we do not know a certain state of the P_c states, we need to choose a decay channel as a reference. We normalized the decay width based on $\Gamma\left(P_c(4312, \frac{1}{2}, \frac{3}{2}) \to NJ\psi\right) = 1$. There are three normalized values for each P_c state, they were calculated by $P_c(4312)$, $P_c(4440)$ and $P_c(4457)$ for the upper, middle and lower values, respectively. Since P_c decays to pJ/ψ channel in experiment, which is isospin $\frac{1}{2}$, we show only the calculation for the isospin $\frac{1}{2}$. The normalized decay width of $j = \frac{3}{2}$ and $j = \frac{1}{2}$ are shown in Table 3.8 and 3.9, respectively.

Table 3.8 Normalized decay width of $\mathbf{j} = \frac{3}{2}$.

P_c configuration	$\Delta^+\eta_c$	$p\eta_c$	Δ^+J/ψ	pJ/ψ	$\Sigma_c^*\bar{D}$	$\Sigma_c\bar{D}$	$\Lambda_c^+\bar{D}$	$\Lambda_c^+\bar{D}^*$	total
$\Psi_{[111]_C[2]_F[3][2]_S}$				1					1
				0.88					0.88
				0.84					0.84
$\Psi_{[111]_C[2]_F[3][11]_S}$				0.60					0.60
				0.53	58.69				59.22
				0.52	59.93				60.45
$\Psi_{[111]_C[2]_F[21][2]_S}$				0.20					0.20
				0.18					0.18
				0.17					0.17
$\Psi_{[111]_C[11]_F[21][2]_S}$				1.80				46.21	48.01
				1.58				58.46	60.04
				1.55				57.42	58.97
$\Psi_{[21]^\rho_C[2]_F[3][2]_S}$				8.01					8.01
				7.01					7.01
				6.89					6.89
$\Psi_{[21]^\rho_C[2]_F[3][11]_S}$				4.80					4.80
				4.21					4.21
				4.13					4.13
$\Psi_{[21]^\rho_C[2]_F[21]^\lambda[2]_S}$				1.60					1.60
				1.40					1.40
				1.38					1.38
$\Psi_{[21]^\rho_C[11]_F[21]^\rho[2]_S}$				14.40					14.40
				12.62					12.62
				12.40					12.40

Table 3.9 Normalized decay width of $\mathbf{j} = \frac{1}{2}$.

P_c configuration	$\Delta^+\eta_c$	$p\eta_c$	$\Delta^+ J/\psi$	pJ/ψ	$\Sigma_c^*\bar{D}$	$\Sigma_c\bar{D}$	$\Lambda_c^+\bar{D}$	$\Lambda_c^+\bar{D}^*$	total
		1.08		0.40					1.48
$\Psi_{[111]_C[2]_F[3][2]_S}$		0.95		0.35					1.30
		0.93		0.34					1.27
		0.13		1.25					1.38
$\Psi_{[111]_C[2]_F[21][2]_S}$		0.12		1.10					1.22
		0.12		1.08					1.20
		0.41		0.15					0.56
$\Psi_{[111]_C[2]_F[21][11]_S}$		0.35		0.13		58.91			59.39
		0.35		0.13		58.11			58.59
		1.22		0.45				46.21	47.88
$\Psi_{[111]_C[11]_F[21][2]_S}$		1.06		0.39				58.46	59.91
		1.04		0.39				57.42	58.85
		0.41		1.35			55.70		57.46
$\Psi_{[111]_C[11]_F[21][11]_S}$		0.35		1.18			47.52		49.05
		0.35		1.16			46.43		47.94
		8.66		3.20					11.86
$\Psi_{[21]^\rho_C[2]_F[3][2]_S}$		7.57		2.80					10.37
		7.43		2.75					10.18
		1.08		10.00					11.08
$\Psi_{[21]^\rho_C[2]_F[21]^\lambda[2]_S}$		0.95		8.77					9.72
		0.94		8.61					9.55
		3.25		1.22					4.47
$\Psi_{[21]^\rho_C[2]_F[21]^\lambda[11]_S}$		2.84		1.05					3.89
		2.79		1.03					3.82
		9.74		3.60					13.34
$\Psi_{[21]^\rho_C[11]_F[21]^\rho[2]_S}$		8.51		3.16					11.67
		8.36		3.10					1.46
		3.25		10.80					14.05
$\Psi_{[21]^\rho_C[11]_F[21]^\rho[11]_S}$		2.84		9.47					12.31
		2.79		9.30					12.09

CHAPTER IV

DISCUSSION AND CONCLUSION

We studied the three charmonium-like pentaquark states, $P_c(4312)$ $P_c(4440)$ and $P_c(4457)$ by using the quark model. We assumed that the pentaquark states are bound states of a baryon-meson molecule. By applying group theory, 47 states for the ground state pentaquark were derived (Table 2.13). We calculated the color-spin-flavor factor to determine the allowed channels (Section 3.3). The factor shows that some pentaquarks in the configuration of color *octet* $\otimes$ *octet* are not open due to the color factor as shown in Appendix A.6. We calculated the transition amplitude for: the direct and cross diagram. Though the spatial wave function is in the Gaussian form for the harmonic oscillator, we used the phenomenological form Eq. (3.9) to calculate the partial decay ratio and the normalized decay width. From the results in Sections 3.4 and 3.5, we find that

- Some pentaquark states in the color *octet* $\otimes$ *octet* configuration dominate the state in the color [111] configuration for the hidden charm decay channels.
- Our results indicate the baryon-meson molecule states decay dominantly through the open charm channels.

For the case of $P_c(4312)$ with spin 3/2, there are only two open decay channels: pJ/ψ, and $\Lambda_c^+\bar{D}^*$ while for the case of spin 1/2, four open decay channels exist: $p\eta_c$, pJ/ψ, Λ_c^+D, and $\Lambda_c^+\bar{D}^*$. The decays to $p\eta_c$, and $\Lambda_c^+\bar{D}$ will be the important decay channels to determine the spin of $P_c(4312)$ since the decay channels open only in the spin 1/2.

Due to their mass being close to each other, $P_c(4440)$ and $P_c(4457)$ have the same decay channels as shown in Table 3.1. The decay channels for spin 3/2 are

pJ/ψ, $\Sigma_c^*\bar{D}$, and $\Lambda_c^+\bar{D}^*$ while the $p\eta_c$, pJ/ψ, $\Sigma_c\bar{D}$, $\Lambda_c^+\bar{D}$, and $\Lambda_c^+\bar{D}^*$ channel open for the spin 1/2. Thus the decay channels of $p\eta_c$, $\Sigma_c\bar{D}$, $\Lambda_c^+\bar{D}$ and $\Sigma_c^*\bar{D}$ could be used to determine the spin of $P_c(4440)$ and $P_c(4457)$. If the pentaquark decays to $p\eta_c$, $\Sigma_c\bar{D}$ and $\Lambda_c^+\bar{D}$, then its spin should be $\frac{1}{2}$ while the decay in $\Sigma_c^*\bar{D}$ would indicate its spin to be $\frac{3}{2}$. However, this is the conclusion when we only consider the pentaquark in the molecular picture. The spin has to be considered in the other models as well. As a result, we strongly suggest that charmonium-like pentaquarks to be searched in experiments in both the open charm and hidden charm channels.

While the investigation of the decay channel leads to the spin of the pentaquark, the ratios sensitively depend on the pentaquark configuration. From Table 3.7 for $I = \frac{1}{2}$ and $j = \frac{1}{2}$, there are three different values of the ratio of $\frac{\Gamma(P_c \to N\eta_c)}{\Gamma(P_c \to NJ/\psi)}$: 2.7, 0.1, and 0.3 while the ratio, to the open charm decay channel for $I = \frac{1}{2}$ and $j = \frac{3}{2}$ are

$$\frac{\Gamma(P_c \to \Sigma_c^*\bar{D})}{\Gamma(P_c \to NJ/\psi)} = 116, \tag{4.1}$$

$$\frac{\Gamma(P_c \to \Lambda_c^+\bar{D})}{\Gamma(P_c \to NJ/\psi)} = 37, \tag{4.2}$$

and for $I = \frac{1}{2}$ and $j = \frac{1}{2}$,

$$\frac{\Gamma(P_c \to \Sigma_c\bar{D})}{\Gamma(P_c \to NJ/\psi)} = 40, \tag{4.3}$$

$$\frac{\Gamma(P_c \to \Lambda_c^+\bar{D})}{\Gamma(P_c \to NJ/\psi)} = 451, \tag{4.4}$$

$$\frac{\Gamma(P_c \to \Lambda_c^+\bar{D})}{\Gamma(P_c \to NJ/\psi)} = 148. \tag{4.5}$$

In this baryon-meson molecular picture, the pentaquark should also be found in the open charm decay channel since the results show that the open charm decay channel strongly dominates over the hidden charm decay channel. On the other

hand, the result from the available experiment shows that the hidden charm decay channel dominates the other channels. Thus P_c is not likely to be a molecule state.

For the other possibilities of the charmonium-like pentaquark state of $I = \frac{3}{2}$, the results in Table 3.6 show that they all decay to $\Delta^+ J/\psi$, although some P_c states can also decay to $\Delta^+ \eta_c$. There are two decay modes in the open charm channel for $I = \frac{3}{2}$ with different spin. For $j = \frac{3}{2}$,

$$\frac{\Gamma(P_c, \to \Sigma_c^* \bar{D})}{\Gamma(P_c, \to \Delta^+ J/\psi)} = 28, \tag{4.6}$$

and for $j = \frac{1}{2}$

$$\frac{\Gamma(P_c \to \Sigma_c \bar{D})}{\Gamma(P_c \to \Delta^+ J/\psi)} = 17. \tag{4.7}$$

For the charmonium-like pentaquark with $I = \frac{3}{2}$, our results show that the open charm decay channel also slightly dominates over the hidden charm decay channel though not as strong as in $I = \frac{1}{2}$.

In summary, our study excluded some of the pentaquark configurations because the color-spin-flavor factor is zero. We have found some decay channels are very promising to determine the spin of the pentaquark experimentally: $p\eta_c$, $\Sigma_c \bar{D}$, $\Sigma_c^* \bar{D}$ and $\Lambda_c^+ \bar{D}$. For experimental observation, the open charm decay channels might be estimated by $BR(\Sigma_c^{(*)} \to \Lambda_c \pi^+) = 100\%$, $BR(\Lambda_c \to pK^-\pi^+) = 5\%$ and $BR(D^+ \to K^-\pi^+\pi^+) = 10\%$ which leads to the decay ratio being multiplied roughly by 0.005. The η_c decay for the hidden charm decay channel might be estimated by $BR(\eta_c \to \gamma\gamma) = 1.58 \times 10^{-4}\%$.

REFERENCES

REFERENCES

Aaij, R., Abellán Beteta, C., Adeva, B., Adinolfi, M., Aidala, C. A., Ajaltouni, Z., Akar, S., Albicocco, P., Albrecht, J., Alessio, F., Alexander, M., Alfonso Albero, A., Alkhazov, G., Alvarez Cartelle, P., and Alves, A. A. et al. (2019). Observation of a Narrow Pentaquark State, $P_c(4312)^+$, and of the Two-Peak Structure of the $P_c(4450)^+$. **Phys. Rev. Lett.** 122 (22): 222001. DOI: 10.1103/PhysRevLett.122.222001. URL: https://link.aps.org/doi/10.1103/PhysRevLett.122.222001.

Aaij, R., Abellán Beteta, C., Adeva, B., Adinolfi, M., Ajaltouni, Z., Akar, S., Albrecht, J., Alessio, F., Alexander, M., Ali, S., Alkhazov, G., Alvarez Cartelle, P., Alves, A. A., Amato, S., Amerio, S., and Amhis, Y. et al. (2016). Model-Independent Evidence for $J/\psi p$ Contributions to $\Lambda_b^0 \to J/\psi p K^-$ Decays. **Phys. Rev. Lett.** 117 (8): 082002. DOI: 10.1103/PhysRevLett.117.082002. URL: https://link.aps.org/doi/10.1103/PhysRevLett.117.082002.

Aaij, R., Adeva, B., Adinolfi, M., Affolder, A., Ajaltouni, Z., Akar, S., Albrecht, J., Alessio, F., Alexander, M., Ali, S., Alkhazov, G., Alvarez Cartelle, P., Alves, A. A., Amato, S., and Amerio, S. et al. (2015). Observation of $J/\psi p$ Resonances Consistent with Pentaquark States in $\Lambda_b^0 \to J/\psi K^- p$ Decays. **Phys. Rev. Lett.** 115 (7): 072001. DOI: 10.1103/PhysRevLett.115.072001. URL: https://link.aps.org/doi/10.1103/PhysRevLett.115.072001.

ATLAS collaboration (Oct. 2019). Study of $J/\psi p$ resonances in the $\Lambda_b^0 \to J/\psi p K^-$ decays in pp collisions at $\sqrt{s}$=7 and 8TeV with the ATLAS detector.

Barnes, V. E., Connolly, P. L., Crennell, D. J., Culwick, B. B., Delaney, W. C., Fowler, W. B., Hagerty, P. E., Hart, E. L., Horwitz, N., Hough, P. V. C., Jensen, J. E., Kopp, J. K., Lai, K. W., Leitner, J., Lloyd, J. L., London, G. W., Morris,

T. W., Oren, Y., Palmer, R. B., Prodell, A. G., Radojicic, D., Rahm, D. C., Richardson, C. R., Samios, N. P., Sanford, J. R., Shutt, R. P., Smith, J. R., Stonehill, D. L., Strand, R. C., Thorndike, A. M., Webster, M. S., Willis, W. J., and Yamamoto, S. S. (1964). Observation of a Hyperon with Strangeness Minus Three. **Phys. Rev. Lett.** 12 (8): 204–206. DOI: 10.1103/PhysRevLett.12.204. URL: https://link.aps.org/doi/10.1103/PhysRevLett.12.204.

Brambilla, Nora, Eidelman, Simon, Hanhart, Christoph, Nefediev, Alexey, Shen, Cheng-Ping, Thomas, Christopher E., Vairo, Antonio, and Yuan, Chang-Zheng (2020). The XYZ states: experimental and theoretical status and perspectives. **Phys. Rept.** 873: 1–154. DOI: 10.1016/j.physrep.2020.05.001. arXiv: 1907.07583 [hep-ex].

Chen, Hua-Xing, Chen, Wei, Liu, Xiang, and Zhu, Shi-Lin (2016). The hidden-charm pentaquark and tetraquark states. **Phys. Rept.** 639: 1–121. DOI: 10.1016/j.physrep.2016.05.004. arXiv: 1601.02092 [hep-ph].

D0 Collaboration (2019). *Inclusive production of the P_c resonances in $p\overline{p}$ collisions.* arXiv: 1910.11767 [hep-ex].

Dover, Carl B., Gutsche, T., Maruyama, M., and Faessler, Amand (1992). The Physics of nucleon - anti-nucleon annihilation. **Prog. Part. Nucl. Phys.** 29: 87–174. DOI: 10.1016/0146-6410(92)90004-L.

Gell-Mann, M. (1964). A schematic model of baryons and mesons. **Physics Letters** 8(3): 214 –215. ISSN: 0031-9163. DOI: https://doi.org/10.1016/S0031-9163(64)92001-3. URL: http://www.sciencedirect.com/science/article/pii/S0031916364920013.

Hosaka, Atsushi, Iijima, Toru, Miyabayashi, Kenkichi, Sakai, Yoshihide, and Yasui, Shigehiro (2016). Exotic hadrons with heavy flavors: X, Y, Z, and related states. **PTEP** 2016(6): 062C01. DOI: 10.1093/ptep/ptw045. arXiv: 1603.09229 [hep-ph].

James, Gordon and Liebeck, Martin (2001). *Representations and Characters of Groups*. **Cambridge University Press**. DOI: 10.1017/CBO9780511814532.

Liu, Yan-Rui, Chen, Hua-Xing, Chen, Wei, Liu, Xiang, and Zhu, Shi-Lin (2019). Pentaquark and Tetraquark states. **Prog. Part. Nucl. Phys.** 107: 237–320. DOI: 10.1016/j.ppnp.2019.04.003. arXiv: 1903.11976 [hep-ph].

Lü, Qi-Fang and Dong, Yu-Bing (2016). Strong decay mode $J/\psi p$ of hidden charm pentaquark states $P_c^+(4380)$ and $P_c^+(4450)$ in $\Sigma_c\overline{D}^*$ molecular scenario. **Phys. Rev. D** 93 (7): 074020. DOI: 10.1103/PhysRevD.93.074020. URL: https://link.aps.org/doi/10.1103/PhysRevD.93.074020.

Nakano, T., Ahn, D. S., Ahn, J. K., Akimune, H., Asano, Y., Chang, W. C., Daté, S., Ejiri, H., Fujimura, H., Fujiwara, M., and al., et (2003). Evidence for a NarrowS=+1Baryon Resonance in Photoproduction from the Neutron. **Physical Review Letters** 91(1). ISSN: 1079-7114. DOI: 10.1103/physrevlett.91.012002. URL: http://dx.doi.org/10.1103/PhysRevLett.91.012002.

Vandermeulen, J. (1988). N ANTI-N ANNIHILATION CREATES TWO MESONS. **Z. Phys. C** 37: 563–567. DOI: 10.1007/BF01549715.

Xu, Kai, Kaewsnod, Attaphon, Liu, Xuyang, Srisuphaphon, Sorakrai, Limphirat, Ayut, and Yan, Yupeng (2019). Complete basis for the pentaquark wave function in a group theory approach. **Phys. Rev. C** 100(6): 065207. DOI: 10.1103/PhysRevC.100.065207. arXiv: 1908.04972 [hep-ph].

Yan, Yupeng (2020). *Applied Group Theory in Physics*. Suranaree University of Technology, Thailand.

Zhu, Shi-Lin (2004). PENTAQUARKS. **International Journal of Modern Physics A** 19(21): 3439–3469. ISSN: 1793-656X. DOI: 10.1142/s0217751x04019676. URL: http://dx.doi.org/10.1142/S0217751X04019676.

Zweig, G. (Feb. 1964). "An SU(3) model for strong interaction symmetry and its breaking. Version 2". *DEVELOPMENTS IN THE QUARK THEORY OF*

HADRONS. VOL. 1. 1964 - 1978. Ed. by D.B. Lichtenberg and Simon Peter Rosen, pp. 22–101.

APPENDICIES

APPENDIX A

A.1 Young tabloid diagram

In the language of permutation groups, each young tabloid represents a conjugacy class of S_n. Thus, if we have worked out all the possible Young tabloids of permutation group S_n, then we know all its conjugacy classes and also the number of the irreducible representations since each conjugacy class corresponds to an irreducible representation of S_n. So we would use the lambda pattern $[\lambda]$ to stand for an irreducible representation of S_n where the dimension of a Young tabloid can be calculated by working out all the possible Young tableaux or Weyl tableaux. For example, the irreducible representations of S_3 with the corresponding Young tableaux and dimensions read,

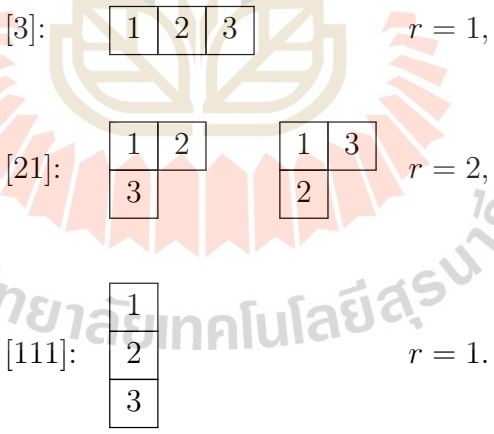

Each representation has a different symmetry, [3] is a symmetric representation, [111] is a antisymmetric representation. The [21] has two dimensions which are mixed symmetric (or so-called λ type, symmetric for the first two particles) and mixed antisymmetric (or so called ρ type, antisymmetric for the first two particles). In the Yamanouchi framework, the number of the basis functions for an irreducible representation corresponds to the number of the Young tableaux. The

basis function can be written as

$$\Phi_{(r)}^{[\lambda]} = |[\lambda](r)\rangle\,, \tag{A.1}$$

where r is the number of box removing for each Young tableaux. The representation matrix for each permutation element can be derived. For S_3, the representation matrix of [3] and [111] has one dimension since both of them have only one Young tableaux while the representation matrix of [21] has two dimensions. For [3], the representation matrices for each permutation element $D^{[3]}(g_i)$ are all equal to 1. For [111], $D^{[111]}(g_i)$ is equal to -1 for (12), (13) and (23) while $D^{[111]}(123) = D^{[111]}(132) = 1$. For [21], Since we know that it has two Young tableaux, the basis function for each Young tableau can be written as

$$\begin{array}{|c|c|}\hline 1 & 2 \\ \hline 3 \\ \cline{1-1}\end{array} \rightarrow \phi_1 = |[21](211)\rangle\,, \qquad \begin{array}{|c|c|}\hline 1 & 3 \\ \hline 2 \\ \cline{1-1}\end{array} \rightarrow \phi_2 = |[21](121)\rangle\,. \tag{A.2}$$

The representation matrix of [21] for the permutation element (12) is

$$D^{[21]}(12) = \sum_{i,j=1}^{2} \langle\phi_j|(12)|\phi_i\rangle = \begin{pmatrix} 1 & 0 \\ 0 & -1 \end{pmatrix}, \tag{A.3}$$

Similarly,

$$D^{[21]}(23) = \begin{pmatrix} -1/2 & \sqrt{3}/2 \\ -\sqrt{3}/2 & 1/2 \end{pmatrix}, \tag{A.4}$$

$$D^{[21]}(13) = D^{[21]}(23)D^{[21]}(12)D^{[21]}(23), \tag{A.5}$$

$$= \begin{pmatrix} -1/2 & -\sqrt{3}/2 \\ -\sqrt{3}/2 & 1/2 \end{pmatrix}, \tag{A.6}$$

$$D^{[21]}(123) = D^{[21]}(13)D^{[21]}(12), \tag{A.7}$$

$$= \begin{pmatrix} -1/2 & -\sqrt{3}/2 \\ \sqrt{3}/2 & -1/2 \end{pmatrix}, \tag{A.8}$$

$$D^{[21]}(132) = D^{[21]}(12)D^{[21]}(13), \tag{A.9}$$

$$= \begin{pmatrix} -1/2 & \sqrt{3}/2 \\ -\sqrt{3}/2 & -1/2 \end{pmatrix}, \tag{A.10}$$

To derive the explicit form of the basis wave function, one can use the method of projection operator. The projection operator of the permutation group S_n takes form

$$W^{[\lambda]}_{(r)} = \frac{n_\lambda}{n!} \sum_i \langle [\lambda](r)|g_i|[\lambda](r)\rangle \, g_i, \tag{A.11}$$

where g_i stand for all the elements of S_n and n_λ is the dimension of the representation $[\lambda]$. Operating $W^{[\lambda]}_{(r)}$ on any function $f(1, 2, \cdots, n)$, one can derive the

corresponding basis function. For example, ϕ_1 of representation [21],

$$\phi_1 = W_1^{[21]} f(123) \tag{A.12}$$
$$= \frac{2}{3!} \sum_i \langle \phi_1 | g_i | \phi_1 \rangle \, g_i f(123) \tag{A.13}$$
$$= \left[\frac{2}{6} \sum_i D_{11}^{[21]} g_i \right] f(132) \tag{A.14}$$
$$= \frac{1}{3} \left[1 + (12) - \frac{1}{2}(13) - \frac{1}{2}(23) - \frac{1}{2}(123) - \frac{1}{2}(132) \right] f(123) \tag{A.15}$$
$$= \frac{1}{3} \left[f(123) + f(213) - \frac{1}{2} f(321) - \frac{1}{2} f(132) - \frac{1}{2} f(231) - \frac{1}{2} f(312) \right]. \tag{A.16}$$

For $SU(n)$ group, the direct product of two irreducible representations of $SU(2)$ or $SU(3)$ is generally reducible. The reduction can be worked out by using the method of the outer product of permutation groups. The irreducible representations can be represented by using the Young tabloid but the dimension for each Young tabloid corresponds to the number of the Weyl tableaux. For $SU(3)$, representations [3], [21] and [111] form a decuplet, octet and singlet, respectively, while for $SU(2)$, [3] and [21] form a 4-multiplet and doublet, respectively, for $SU(2)$, there is no representation [111].

A.2 Applied orthogonal theorem

The character of the product of irreducible representations can be written as

$$\chi(g) = \chi^{(\alpha)}(g) \chi^{(\beta)}(g), \tag{A.17}$$

while the character of reducible representation can be written as

$$\chi(g) = \sum_{\sigma} m_{(\sigma)} \chi^{(\sigma)}(g). \tag{A.18}$$

The α and β irreducible representation correspond to the γ irreducible representation can be calculated from

$$\langle \chi^{(\gamma)}, \chi \rangle = \sum_{\sigma} m_{(\sigma)} \langle \chi^{(\gamma)}, \chi^{(\sigma)} \rangle = \langle \chi^{(\gamma)}, \chi^{(\alpha)} \chi^{(\beta)} \rangle, \tag{A.19}$$

$$m_{(\sigma)} \delta_{\gamma,\sigma} = \frac{1}{n} \sum_{g} \chi^{(\gamma)*}(g) \left(\chi^{(\alpha)}(g) \chi^{(\beta)}(g) \right), \tag{A.20}$$

$$m_{(\gamma)} = \frac{1}{n} \sum_{i} \rho_i \chi_i^{(\gamma)*} \left(\chi_i^{(\alpha)} \chi_i^{(\beta)} \right), \tag{A.21}$$

where $\sum_i$ is sum over conjugacy class i, ρ_i is number of group element in the conjugacy class i.

A.3 Wave function combination

To determine the coefficients $a_{i,j}$ in Eqs. (2.4), (2.7), (2.8) and (2.9) in Subsection 2.1.1 or Eq. (2.27) in Section 2.3, one needs to apply the permutation operator according to the irreducible representation. Here we show the example of the octet baryon for the spin-flavor configuration. The wave function of baryon octet for the ground state can be written as

$$\Psi = \psi^c_{[111]} \psi^o_S \psi^{sf}_S. \tag{A.22}$$

The spin-flavor wave function in the case of baryon octet can be written as

$$\psi^{sf}_S = \sum_{i,j=\lambda,\rho} a_{i,j} \psi^s_{[21]_i} \psi^f_{[21]_j}. \tag{A.23}$$

Applying (12) permutation,

$$(12)\psi_S^{sf} = \psi_S^{sf} = a_{\lambda,\lambda}\psi^s_{[21]_\lambda}\psi^f_{[21]_\lambda} - a_{\lambda,\rho}\psi^s_{[21]_\lambda}\psi^f_{[21]_\rho} - a_{\rho,\lambda}\psi^s_{[21]_\rho}\psi^f_{[21]_\lambda} + a_{\rho,\rho}\psi^s_{[21]_\rho}\psi^f_{[21]_\rho}. \tag{A.24}$$

Since the ψ_S^{sf} must transform as symmetric, this require $a_{\lambda,\rho} = a_{\rho,\lambda} = 0$. Thus,

$$\psi_S^{sf} = a_{\lambda,\lambda}\psi^s_{[21]_\lambda}\psi^f_{[21]_\lambda} + a_{\rho,\rho}\psi^s_{[21]_\rho}\psi^f_{[21]_\rho}. \tag{A.25}$$

Applying (23) permutation,

$$\begin{aligned}(23)\psi_S^{sf} = \psi_S^{sf} =& a_{\lambda,\lambda}(-\frac{1}{2}\psi^s_{[21]_\lambda} + \frac{\sqrt{3}}{2}\psi^s_{[21]_\rho})(-\frac{1}{2}\psi^f_{[21]_\lambda} + \frac{\sqrt{3}}{2}\psi^f_{[21]_\rho}) \\ &+ a_{\rho,\rho}(\frac{\sqrt{3}}{2}\psi^s_{[21]_\lambda} + \frac{1}{2}\psi^s_{[21]_\rho})(\frac{\sqrt{3}}{2}\psi^f_{[21]_\lambda} + \frac{1}{2}\psi^f_{[21]_\rho}).\end{aligned} \tag{A.26}$$

Solving Eq. (A.26) by substitute Eq. (A.25), the result is $a_{\lambda,\lambda} = a_{\rho,\rho}$. So the spin-flavor wave function of the octet baryon can be written by

$$\psi_S^{sf} = \frac{1}{\sqrt{2}}(\psi^s_\lambda\psi^f_\lambda + \psi^s_\rho\psi^f_\rho). \tag{A.27}$$

The representation matrix for the [21] irreducible representation of S_3 are

$$D^{[21]}(12) = \begin{pmatrix} 1 & 0 \\ 0 & -1 \end{pmatrix}, \quad D^{[21]}(23) = \begin{pmatrix} -1/2 & \sqrt{3}/2 \\ -\sqrt{3}/2 & 1/2 \end{pmatrix}, \tag{A.28}$$

and

$$D^{[21]}(13) = D^{[21]}(23)D^{[21]}(12)D^{[21]}(23), \tag{A.29}$$

$$D^{[21]}(123) = D^{[21]}(13)D^{[21]}(12), \tag{A.30}$$

$$D^{[21]}(132) = D^{[21]}(12)D^{[21]}(13). \tag{A.31}$$

For representation [3], the representation matrices are 1 for all the elements while the representation matrices of [111] are equal to -1 for (12), (13) and (23), and equal to 1 for (123) and (132).

A.4 Coupling the flavor wave function

Since we consider only u and d quark, the coupling of flavor and spin wave function can be calculated by using Clebsch-Gordan coefficients.

$$\left|j^{P_c}, m\right\rangle = \sum_{m_1,m_2} CG[j^B, m_1, j^M, m_2, j, m_i + m_j] \left|j^B, m_1\right\rangle \left|j^M, m_2\right\rangle . \tag{A.32}$$

$\frac{3}{2} \otimes 0$

$$\left|\phi, \frac{3}{2}, \frac{1}{2}\right\rangle = \left|\frac{3}{2}, \frac{1}{2}\right\rangle |0, 0\rangle \tag{A.33}$$

$\frac{1}{2}^{\alpha} \otimes 0$

$\alpha = [21]_\lambda$, $[21]_\rho$.

$$\left|\phi_\alpha, \frac{1}{2}, \frac{1}{2}\right\rangle = \left|\frac{1}{2}^{\alpha}, \frac{1}{2}\right\rangle |0, 0\rangle \tag{A.34}$$

$1 \otimes \frac{1}{2}$

$$\left|\phi_1, \frac{3}{2}, \frac{1}{2}\right\rangle = \frac{1}{\sqrt{3}} |1, 1\rangle \left|\frac{1}{2}, -\frac{1}{2}\right\rangle + \sqrt{\frac{2}{3}} |1, 0\rangle \left|\frac{1}{2}, \frac{1}{2}\right\rangle \tag{A.35}$$

$$\left|\phi_1, \frac{1}{2}, \frac{1}{2}\right\rangle = \sqrt{\frac{2}{3}} |1, 1\rangle \left|\frac{1}{2}, -\frac{1}{2}\right\rangle - \frac{1}{\sqrt{3}} |1, 0\rangle \left|\frac{1}{2}, \frac{1}{2}\right\rangle \tag{A.36}$$

$0 \otimes \frac{1}{2}$

$$\left|\phi_0, \frac{1}{2}, \frac{1}{2}\right\rangle = \left|\phi^B, 0, 0\right\rangle \left|\phi^M, \frac{1}{2}, \frac{1}{2}\right\rangle \tag{A.37}$$

A.5 Coupling spin wave function

We show all the possible spin couplings between the baryon and meson part for the pentaquark.

$\frac{3}{2} \otimes 1$

$$\left|\chi, \frac{5}{2}, \frac{5}{2}\right\rangle = \left|\frac{3}{2}, \frac{3}{2}\right\rangle |1, 1\rangle \tag{A.38}$$

$$\left|\chi, \frac{5}{2}, \frac{3}{2}\right\rangle = \sqrt{\frac{2}{5}} \left|\frac{3}{2}, \frac{3}{2}\right\rangle |1, 0\rangle + \sqrt{\frac{3}{5}} \left|\frac{3}{2}, \frac{1}{2}\right\rangle |1, 1\rangle \tag{A.39}$$

$$\left|\chi, \frac{5}{2}, \frac{1}{2}\right\rangle = \frac{1}{\sqrt{10}} \left|\frac{3}{2}, \frac{3}{2}\right\rangle |1, -1\rangle + \sqrt{\frac{3}{5}} \left|\frac{3}{2}, \frac{1}{2}\right\rangle |1, 0\rangle + \sqrt{\frac{3}{10}} \left|\frac{3}{2}, -\frac{1}{2}\right\rangle |1, 1\rangle \tag{A.40}$$

$$\left|\chi, \frac{5}{2}, -\frac{1}{2}\right\rangle = \sqrt{\frac{3}{10}} \left|\frac{3}{2}, \frac{1}{2}\right\rangle |1, -1\rangle + \sqrt{\frac{3}{5}} \left|\frac{3}{2}, -\frac{1}{2}\right\rangle |1, 0\rangle + \frac{1}{\sqrt{10}} \left|\frac{3}{2}, -\frac{3}{2}\right\rangle |1, 1\rangle \tag{A.41}$$

$$\left|\chi, \frac{5}{2}, -\frac{3}{2}\right\rangle = \sqrt{\frac{3}{5}} \left|\frac{3}{2}, -\frac{1}{2}\right\rangle |1, -1\rangle + \sqrt{\frac{2}{5}} \left|\frac{3}{2}, -\frac{3}{2}\right\rangle |1, 0\rangle \tag{A.42}$$

$$\left|\chi, \frac{5}{2}, -\frac{5}{2}\right\rangle = \left|\frac{3}{2}, -\frac{3}{2}\right\rangle |1, -1\rangle \tag{A.43}$$

(A.44)

$$\left|\chi,\frac{3}{2},\frac{3}{2}\right\rangle = \sqrt{\frac{3}{5}}\left|\frac{3}{2},\frac{3}{2}\right\rangle|1,0\rangle - \sqrt{\frac{2}{5}}\left|\frac{3}{2},\frac{1}{2}\right\rangle|1,1\rangle \tag{A.45}$$

$$\left|\chi,\frac{3}{2},\frac{1}{2}\right\rangle = \sqrt{\frac{2}{5}}\left|\frac{3}{2},\frac{3}{2}\right\rangle|1,-1\rangle + \frac{1}{\sqrt{15}}\left|\frac{3}{2},\frac{1}{2}\right\rangle|1,0\rangle - 2\sqrt{\frac{2}{15}}\left|\frac{3}{2},-\frac{1}{2}\right\rangle|1,1\rangle \tag{A.46}$$

$$\left|\chi,\frac{3}{2},-\frac{1}{2}\right\rangle = 2\sqrt{\frac{2}{15}}\left|\frac{3}{2},\frac{1}{2}\right\rangle|1,-1\rangle - \frac{1}{\sqrt{15}}\left|\frac{3}{2},-\frac{1}{2}\right\rangle|1,0\rangle - \sqrt{\frac{2}{5}}\left|\frac{3}{2},-\frac{3}{2}\right\rangle|1,1\rangle \tag{A.47}$$

$$\left|\chi,\frac{3}{2},-\frac{3}{2}\right\rangle = \sqrt{\frac{2}{5}}\left|\frac{3}{2},-\frac{1}{2}\right\rangle|1,-1\rangle - \sqrt{\frac{3}{5}}\left|\frac{3}{2},-\frac{3}{2}\right\rangle|1,0\rangle \tag{A.48}$$

(A.49)

$$\left|\chi,\frac{1}{2},\frac{1}{2}\right\rangle = \frac{1}{\sqrt{2}}\left|\frac{3}{2},\frac{3}{2}\right\rangle|1,-1\rangle - \frac{1}{\sqrt{3}}\left|\frac{3}{2},\frac{1}{2}\right\rangle|1,0\rangle + \frac{1}{\sqrt{6}}\left|\frac{3}{2},-\frac{1}{2}\right\rangle|1,1\rangle \tag{A.50}$$

$$\left|\chi,\frac{1}{2},-\frac{1}{2}\right\rangle = \frac{1}{\sqrt{6}}\left|\frac{3}{2},\frac{1}{2}\right\rangle|1,-1\rangle - \frac{1}{\sqrt{3}}\left|\frac{3}{2},-\frac{1}{2}\right\rangle|1,0\rangle + \frac{1}{\sqrt{2}}\left|\frac{3}{2},-\frac{3}{2}\right\rangle|1,1\rangle \tag{A.51}$$

$\frac{1}{2}^{\alpha} \otimes 1$

$\alpha = [21]_{\lambda},\ [21]_{\rho}.$

$$\left|\chi_{\alpha},\frac{3}{2},\frac{3}{2}\right\rangle = \left|\frac{1}{2}^{\alpha},\frac{1}{2}\right\rangle|1,1\rangle \tag{A.52}$$

$$\left|\chi_{\alpha},\frac{3}{2},\frac{1}{2}\right\rangle = \sqrt{\frac{2}{3}}\left|\frac{1}{2}^{\alpha},\frac{1}{2}\right\rangle|1,0\rangle + \frac{1}{\sqrt{3}}\left|\frac{1}{2}^{\alpha},-\frac{1}{2}\right\rangle|1,1\rangle \tag{A.53}$$

$$\left|\chi_{\alpha},\frac{3}{2},-\frac{1}{2}\right\rangle = \frac{1}{\sqrt{3}}\left|\frac{1}{2}^{\alpha},\frac{1}{2}\right\rangle|1,-1\rangle + \sqrt{\frac{2}{3}}\left|\frac{1}{2}^{\alpha},-\frac{1}{2}\right\rangle|1,0\rangle \tag{A.54}$$

$$\left|\chi_{\alpha},\frac{3}{2},-\frac{3}{2}\right\rangle = \left|\frac{1}{2}^{\alpha},-\frac{1}{2}\right\rangle|1,-1\rangle \tag{A.55}$$

$$\left|\chi_\alpha, \frac{1}{2}^\alpha, \frac{1}{2}\right\rangle = \frac{1}{\sqrt{3}}\left|\frac{1}{2}^\alpha, \frac{1}{2}\right\rangle |1,0\rangle - \sqrt{\frac{2}{3}}\left|\frac{1}{2}^\alpha, -\frac{1}{2}\right\rangle |1,1\rangle \tag{A.56}$$

$$\left|\chi_\alpha, \frac{1}{2}^\alpha, -\frac{1}{2}\right\rangle = \sqrt{\frac{2}{3}}\left|\frac{1}{2}^\alpha, \frac{1}{2}\right\rangle |1,-1\rangle - \frac{1}{\sqrt{3}}\left|\frac{1}{2}^\alpha, -\frac{1}{2}\right\rangle |1,0\rangle \tag{A.57}$$

(A.58)

$\frac{3}{2} \otimes 0$

$$\left|\chi_0, \frac{3}{2}, m\right\rangle = \left|\frac{3}{2}, m\right\rangle |0,0\rangle \tag{A.59}$$

$\frac{1}{2}^\alpha \otimes 0$

$$\left|\chi_{\alpha 0}, \frac{1}{2}, m\right\rangle = \left|\frac{1}{2}^\alpha, m\right\rangle |0,0\rangle \tag{A.60}$$

A.6 Color-flavor-spin factor

As shown in the straight diagram, the final particle state should be the same as the pentaquark state. Thus the color-flavor-spin factor of the straight diagram has only one value. Here we show the calculation of the color-flavor-spin factor for the cross diagram.

Color factor

We calculate the color factor direclty,

$$\left\langle \psi^B_{[111]} \otimes \psi^M_{[111]} \middle| \psi^{P_c}_{[111]} \right\rangle = \frac{1}{3} \tag{A.61}$$

$$\left\langle \psi^B_{[111]} \otimes \psi^M_{[111]} \middle| \psi^{P_c}_{[21]_\lambda} \right\rangle = 0 \tag{A.62}$$

$$\left\langle \psi^B_{[111]} \otimes \psi^M_{[111]} \middle| \psi^{P_c}_{[21]_\rho} \right\rangle = \frac{2\sqrt{2}}{3} \tag{A.63}$$

Flavor factor

From the flavor wave function in the Section: Coupling flavor wave function,

we calculated the flavor factor of the cross diagram.

$$\left\langle \phi^F, \frac{3}{2}, \frac{1}{2} \middle| \phi_1^{P_c}, \frac{3}{2}, \frac{1}{2} \right\rangle = 1 \tag{A.64}$$

$$\left\langle \phi^F_{[21]_\lambda}, \frac{1}{2}, \frac{1}{2} \middle| \phi_1^{P_c}, \frac{1}{2}, \frac{1}{2} \right\rangle = 1 \tag{A.65}$$

$$\left\langle \phi^F_{[21]_\rho}, \frac{1}{2}, \frac{1}{2} \middle| \phi_0^{P_c}, \frac{1}{2}, \frac{1}{2} \right\rangle = 1 \tag{A.66}$$

where F refers to to the final state.

Spin factor

The spin factor can be calculated by the Wigner's 9-j symbols. Since the 9-j symbols does not depend on the spin projection, we show the spin factor for each the possible total spin.

$$\left\langle \chi^F, \frac{5}{2}, m \middle| \chi^{P_c}, \frac{5}{2}, m \right\rangle = 1 \tag{A.67}$$

Table A.1 $9-j$ symbols values for $\mathbf{j} = 3/2$

	$\lvert\chi^{P_c}, \frac{3}{2}, m\rangle$	$\lvert\chi^{P_c}_{[21]_\lambda}, \frac{3}{2}, m\rangle$	$\lvert\chi^{P_c}_{[21]_\rho}, \frac{3}{2}, m\rangle$	$\lvert\chi^{P_c}_0, \frac{3}{2}, m\rangle$
$\langle\chi^F, \frac{3}{2}, m\rvert$	$\frac{1}{6}$	$\frac{\sqrt{5}}{3}$	0	$\frac{\sqrt{\frac{5}{3}}}{2}$
$\langle\chi^F_{[21]_\lambda}, \frac{3}{2}, m\rvert$	$\frac{\sqrt{5}}{3}$	$\frac{1}{3}$	0	$-\frac{1}{\sqrt{3}}$
$\langle\chi^F_{[21]_\rho}, \frac{3}{2}, m\rvert$	0	0	1	0
$\langle\chi^F_0, \frac{3}{2}, m\rvert$	$\frac{\sqrt{\frac{5}{3}}}{2}$	$-\frac{1}{\sqrt{3}}$	0	$\frac{1}{2}$

Table A.2 $9-j$ symbols values for $\mathbf{j} = 1/2$

	$\lvert\chi^{P_c}, \frac{1}{2}, m\rangle$	$\lvert\chi^{P_c}_{[21]_\lambda}, \frac{1}{2}, m\rangle$	$\lvert\chi^{P_c}_{[21]_\rho}, \frac{1}{2}, m\rangle$	$\lvert\chi^{P_c}_{[21]_\lambda 0}, \frac{1}{2}, m\rangle$	$\lvert\chi^{P_c}_{[21]_\rho 0}, \frac{1}{2}, m\rangle$
$\langle\chi^F, \frac{1}{2}, m\rvert$	$-\frac{1}{3}$	$\frac{\sqrt{2}}{3}$	0	$\sqrt{\frac{2}{3}}$	0
$\langle\chi^F_{[21]_\lambda}, \frac{1}{2}, m\rvert$	$\frac{\sqrt{2}}{3}$	$\frac{5}{6}$	0	$-\frac{1}{2\sqrt{3}}$	0
$\langle\chi^F_{[21]_\rho}, \frac{1}{2}, m\rvert$	0	0	$-\frac{1}{2}$	0	$\frac{\sqrt{3}}{2}$
$\langle\chi^F_{[21]_\lambda 0}, \frac{1}{2}, m\rvert$	$\sqrt{\frac{2}{3}}$	$-\frac{1}{2\sqrt{3}}$	0	$\frac{1}{2}$	0
$\langle\chi^F_{[21]_\rho 0}, \frac{1}{2}, m\rvert$	0	0	$\frac{\sqrt{3}}{2}$	0	$\frac{1}{2}$

CURRICULUM VITAE

NAME: KANOKPHON PHUMPHAN **GENDER**: Male

NATIONALITY: Thai **DATE OF BIRTH**: APRIL 10, 1995

E-MAIL: k.phoompan393@hotmail.com

EDUCATIONS:

- 2006 - 2011, Assumption College Nakhonratchasima
- 2012 - 2015, Bachelor of Science, Physics department, Institute of science, Khon Kaen University
- 2016 - 2020, Master of Science, School of Physics, Institute of Science, Suranaree University of Technology
- 2019 - 2020, Double/Dual degree program between National Cheng Kung University and Suranaree Universuty of Technology, Master of Science, Department of Physics, College of Science, National Cheng Kung University

EXPERIENCES

- 2019, Participated in 15th Rencontres du Vietnam, Vietnam School on Neutrinos, ICISE center, Quy Nhon, Vietnam.